AN INVESTIGATION OF SURGING IN A COMPRESSOR

JOSEPH FRANCIS BOLGER, JR.
AND
ROBERT EDGAR BURRELL

1953

AN INVESTIGATION OF SURGING IN A COMPRESSOR

by

JOSEPH FRANCIS BOLGER, JR.
B.S., United States Naval Academy
(1945)
B.S., Aeronautical Engineering
United States Naval Postgraduate School
(1952)

and

ROBERT EDGAR BURRELL
B.S., Mechanical Engineering
University of Michigan
(1944)
B.S., Aeronautical Engineering
United States Naval Postgraduate School
(1952)

SUBMITTED IN PARTIAL FULFILLMENT OF THE REQUIREMENTS
FOR THE DEGREE OF MASTER OF SCIENCE
IN AERONAUTICAL ENGINEERING

at the

MASSACHUSETTS INSTITUTE OF TECHNOLOGY
(1953)

Abstract

AN INVESTIGATION OF SURGING IN A COMPRESSOR

by

J. F. Bolger, Jr., Lt., United States Navy

R. E. Burrell, Lt., United States Navy

(Submitted to the Department of Aeronautical Engineering on May 25, 1953, in partial fulfillment of the requirements for the degree of Master of Science.)

An analysis demonstrating a method by which the criterion for stability of a compressor system may be expressed in a simplified form was shown to be applicable to investigation by means of an hydraulic analogue.

The required experimental hydraulic set-up was designed and constructed. An initial investigation of the characteristics obtained by several selected impeller modifications was carried out. The data obtained indicated poor pressure recovery characteristics, which prevented operation in the unstable range.

The investigation was conducted by the authors at the Gas Turbine Laboratory, Massachusetts Institute of Technology, between October 1952 and May 1953.

Thesis Supervisor: Edward S. Taylor

Title: Professor of Aircraft Engines

Cambridge, Massachusetts
May 25, 1953

Professor Shatswell Ober, Chairman
Department Committee on Graduate Students
Department of Aeronautical Engineering
Massachusetts Institute of Technology
Cambridge, Massachusetts

Dear Sir:

In partial fulfillment of the requirements for the degree of Master of Science in Aeronautical Engineering, we herewith submit a thesis entitled "An Investigation of Surging in a Compressor".

Acknowledgments

The authors wish to express their gratitude to Professor Edward S. Taylor and his staff for their help and suggestions in the development of this investigation, and to the staff of the Gas Turbine Laboratory for their cooperation and assistance.

TABLE OF CONTENTS

TABLES (Continued)

XII. Figures

1. Performance curve for a typical centrifugal compressor.
2. Compressor diagrammatic test setup.
3. Analog of compressor setup.
4. Orifice characteristics.
5. Compressor characteristics.
6. Hydraulic analog.
7. $p_3 = \frac{M_a R T_3}{V_{a_3}} + \frac{\rho g V_{w_3}}{A_3}$
8. Linearization near equilibrium point.
9. Schematic experimental test setup.

9a. View of experimental test setup.

10. Experimental curves for impeller with backward curved blades.
11. Experimental curves for impeller with forward curved blades.
12. Experimental curves for impeller with forward curved blades. and inducers.
13. View of impeller.
14. View of opened casing and impeller.
15. Typical characteristic curves for a centrifugal pump.
16. View of impeller with inducers attached.
17. Entrance velocity diagram for DeLaval impeller.
18. Summary of experimental curves.
19. Centrifugal pump characteristics.
20. Outlet velocity diagrams.
21. Radial-vaned impeller design.
22. Conditions for a stable Q-H curve

Figures (Continued)

II. Introduction

It is well known that if at any fixed speed of a compressor, either axial or centrifugal, the flow is reduced by throttling the outlet, then a point is eventually reached at which a complete breakdown of the airflow occurs. In most cases an actual reversal of airflow through the compressor takes place. Sometimes the phenomena occurs gradually in the form of mild bubbling, but more often the occurrence is violent and is of such a magnitude that the compressor may be endangered. In most centrifugal compressors the flow reversal which takes place stops rapidly, the performance recovers, and a second surge occurs if the throttling is not reduced. The frequency of the individual surges varies' according to the amount of throttling and many other conditions; it may be only one isolated occurrence, which would indicate that the working point was just, but only just at the surge point, or it may take the form of a rapid series of surges indicating that the working point is beyond the surge. Normal performance of the compressor may be restored by reduction of throttling.

In order to better understand the phenomenon it is a help to have available some typical performance curves for a compressor of this type. Figure 1 is a plot of volume delivery Q in cubic feet per minute versus the delivery pressure and the compressor tip speed is contained as the parameter. Examining this figure it can be seen that the curves for different tip speed all end on the dotted line known as the surge line which occurs at or just before the maximum pressure occurs. It

follows then, that any one machine is good for only a certain range of flow, namely from the surge point to the critical flow point.

The elements of surge can be explained in the following manner. If surge could be prevented and the performance curve extended to a zero delivery flow, it would be as shown in the dashed extension of Y feet per second tip speed in Figure 1, the pressure reducing below the maximum as the flow delivery approached zero. Suppose the compressor to be operating at the surge point and consider the effect of some transient variable such as a speed fluctuation or a rate of change of flow to occur. Then instantaneously the compressor may be required to deliver a flow below the surge limit, a point such as A where the pressure produced p_A is less than the pressure p_S at the surge point. Examining these conditions, it is seen that there is a considerable volume on the discharge side of the compressor already at pressure p_S and acted on at the discharge area only by pressure p_A. Backflow from the delivery to the suction side of the compressor will occur. For this to occur, the rate of delivery must pass through zero before the flow can reverse, hence the pressure of delivery will travel along the dashed line until point B is reached. The delivery volume then blows down to pressure p_B. Forward flow through the compressor begins at Q_c, the pressure p_c being equal to p_B. This flow rate is in excess of the demand Q_s

and the flow rate hence backs up the curve to the surge point once again. If no transients occur the point is stable. However, if the transients are present the cycle will repeat itself again in the same manner.

It is obvious that such a cycle of events may be accompanied by large scale vibrations and by a serious loss of efficiency. It is the object of this paper to investigate this phenomena of surging in a compressor by means of a water analog.

Examination of Stability

The following work is essentially a reproduction of that of Prof. E. S. Taylor in Ref. 1.

Figure 2 represents a centrifugal air compressor diagrammatic test setup. The throttle valve is provided to regulate pressure across the compressor. The plenum chamber provides an excellent space to measure temperature and pressure and serves to represent that space devoted to combustion chambers in the actual gas turbine.

The following simplified assumptions are made to reduce the complexity of the problem.

1) The density at any point in the compressor is a function of position only for a particular running condition of the compressor. With this assumption, mass flow out of the compressor equals mass flow into the compressor at any instant.

2) Consider the process in the plenum to be isothermal.

3) The pressure versus flow characteristic of the compressor is not affected by transient phenomena, or in other words, the compressor is assumed to be in a quasi-steady state of operation at all times.

4) Friction forces are independent of time.

Figure 3 represents a simplified system based on the above assumptions. The static pressure flow characteristic

of the compressor is supplied by an actuator between section (1) and (2). The compressor is replaced by this actuator and a straight pipe in which flow is incompressible and which is proportioned so that the rate of change of mass flow through the pipe produced by a pressure difference at the ends is the same as the rate of change of mass flow through the compressor for the same value of pressure difference (i.e., difference between the discharge pressure of the compressor and the pressure for equilibrium).

It may be shown that the pipe will be dynamically similar to the compressor if

$$\left(\frac{l}{A\rho}\right)_{pipe} = \int_l \left(\frac{dl}{A\rho}\right)_{compressor} \qquad (1)$$

where l is taken in the flow direction and with no wheel rotation, A is the cross sectional area in a plane perpendicular to the direction of l, and ρ is the density at any point.

Writing the equation of motion ($F = M_a$) in the pipe in the following manner

$$\left[p_1\left(\frac{p_2}{p_1}\right) - p_3\right]A = \frac{\rho A l}{g_o}\frac{du}{dt} \qquad (2)$$

where p_1, p_2 and p_3 are pressures as shown in Fig 3

A is the cross sectional area of the pipe

ρ is the density in the pipe

l is the length of the pipe

u is the velocity in the pipe (assumed uniform throughout pipe).

Since $u = \frac{M_c}{\rho A}$ where M_c is the mass flow through the pipe (compressor) equation (1) may be written in dimensionless form

$$\frac{p_2}{p_1} - \frac{p_3}{p_1} = T \frac{d}{dt}\left(\frac{m_c}{m^*}\right) \tag{3}$$

where the characteristic time T of the compressor is given by

$$T = k \left(\frac{2}{k+1}\right)^{\frac{k+1}{2k-2}} \frac{\pi r_2^2}{A} \frac{\ell}{a_{01}} \tag{4}$$

where k = ratio of specific heats

r_2 = outer radius of impellor

a_{o_1} = velocity of sound at inlet stagnation temperature.

Assuming that the process in the plenum is isothermal (for the sake of simplicity) the rate of change of pressure in the plenum may be written in the dimensionless form

$$\frac{d}{dt}\left(\frac{p_2}{p_1}\right) = F\left(\frac{m_c}{m^*} - \frac{m_o}{m^*}\right) \tag{5}$$

where M_o is the mass flow per unit time in the orifice and the characteristic frequency F of the plenum is given by

$$F = \frac{T_{02}}{T_{01}} \left(\frac{2}{k+1}\right)^{\frac{k+1}{2k-2}} \frac{\pi r_2^2}{V^{2/3}} \frac{a_{01}}{V^{1/3}} \tag{6}$$

where V = volume of the plenum

T_{o_2} = stagnation temperature at compressor outlet

T_{o_1} = stagnation temperature at compressor inlet

There are two further relationships expressing, respectively, the characteristic of the compressor

$$\frac{p_2}{p_1} = f_1\left(\frac{m_c}{m^*}\right) \tag{7}$$

and the characteristic of the orifice

$$\frac{p_3}{p_1} = f_2\left(\frac{m_o}{m^*}\right) \tag{8}$$

The flow through the orifice is considered to respond instantaneously to changes in pressure. Fig. 4 is a plot of f_2 for a converging nozzle of unity coefficient. Fig. 5 is a typical plot of f_1, the compressor characteristic.

These functions are in general complicated and when substituted in equations (3) and (5) will result in non-linear equations which have no analytical solution since equation (6) represents an experimental function. For the purpose of studying stability to small disturbances, it suffices to replace equations (7) and (8) with linear relationships near the equilibrium point, provided that in the near region of this point the two functions are continuous and have first derivatives that are also continuous. The equilibrium point is defined by the relation

$$\left(\frac{p_2}{p_1}\right)_{eq.} = \left(\frac{p_3}{p_1}\right)_{eq.} \tag{9}$$

and

$$\left(\frac{m_o}{m^*}\right)_{eq.} = \left(\frac{m_c}{m^*}\right)_{eq.} \tag{10}$$

With these assumptions, equations (7) and (8) can be written

$$\xi_1 = X \eta_1 \tag{11}$$

$$\xi_2 = Y \eta_2 \tag{12}$$

where

$$\xi_1 = \frac{p_2}{p_1} - \left(\frac{p_2}{p_1}\right)_{eq.} \tag{13}$$

$$\xi_2 = \frac{p_3}{p_1} - \left(\frac{p_3}{p_1}\right)_{eq.} \tag{14}$$

$$\eta_1 = \frac{m_c}{m^*} - \left(\frac{m_c}{m^*}\right)_{eq.} \tag{15}$$

$$\eta_2 = \frac{m_o}{m^*} - \left(\frac{m_o}{m^*}\right)_{eq.} \tag{16}$$

$$X = f'\left(\frac{m_c}{m^*}\right) \text{ at } \left(\frac{m_c}{m^*}\right)_{eq.} \tag{17}$$

$$Y = f'\left(\frac{m_o}{m^*}\right) \text{ at } \left(\frac{m_o}{m^*}\right)_{eq.} \tag{18}$$

It will be seen that X and Y are the slopes of the characteristic curves of the compressor and orifice at the equilibrium point.

Using the new variables ξ and η, equations (3) and (5) can be rewritten:

$$\xi_1 - \xi_2 = T \frac{d}{dt}(\eta_1) \tag{19}$$

$$\frac{d}{dt}(\xi_2) = F(\eta_1 - \eta_2) \tag{20}$$

By substitution of values from (11) and (12) equations (19) and (20) become

$$X\eta_1 - Y\eta_2 = T \frac{d}{dt}(\eta_1) \tag{21}$$

$$Y \frac{d}{dt}(\eta_2) = F(\eta_1 - \eta_2) \tag{22}$$

A solution of equations (21) and (22) is

$$\eta_1 = c_1 e^{bt}$$

$$\eta_2 = c_2 e^{bt}$$

where C_1 and C_2 are arbitrary constants and b is given by the quadratic

$$b^2 + \left(\frac{F}{Y} - \frac{X}{T}\right)b + \frac{F}{T} - \frac{FX}{TY} = 0 \tag{23}$$

of which the roots are

$$b = -\frac{1}{2}\left(\frac{F}{Y} - \frac{X}{T}\right) \mp \sqrt{\frac{1}{4}\left(\frac{F}{Y} - \frac{X}{T}\right)^2 + \frac{F}{T}\left(\frac{X}{Y} - 1\right)} \tag{24}$$

b may be real or complex and the criterion for stability is that the real part of b must not be positive for either root.

If b is complex the variation in ξ is oscillitory and stability is indicated when and only when

$$\frac{F}{Y} - \frac{X}{T} > 0 \tag{25}$$

If b is real, stability is indicated when and only when

$$\frac{F}{Y} - \frac{X}{T} > 0$$

and the radical is not larger in absolute value than the first term in equation (23), that is when

$$\frac{F}{T}\left(\frac{X}{Y} - 1\right) < 0 \qquad (26)$$

The terms Y, F, and T are always positive quantities and therefore equation (24) may be written

$$X < \frac{FT}{Y} > 0 \qquad (27)$$

and equation (28) gives

$$X < Y \qquad (28)$$

Therefore stability is assured if X is negative. This corresponds to saying that a compressor with a falling pressure-flow characteristic will always be stable. A rising characteristic is also stable if the slope X is sufficiently small. How large the slope can be and still maintain stability depends upon the circuit into which the compressor is installed. The smaller the volume of the plenum, the larger the permissible slope of the compressor characteristic. Also, the smaller the slope of the orifice characteristic may be with the exception that if $X > Y$ instability will always result.

The equation derived by Prof. E. S. Taylor apply to a gaseous fluid. However, the problem is not restricted to gases as such phenomena occur in hydraulic systems containing a compressor with pressure-flow characteristics similar to those of Fig. 5. The equations for a water system follow.

Once again simplifying assumptions are made in order to reduce the complexity of the problem.

1) The density at any point in the system is a constant, hence mass flow into the compressor equals mass flow out of the compressor.

2) Consider the process in the plenum to be isothermal.

3) The pressure-flow characteristic of the compressor is not affected by transient phenomena.

4) Friction forces are independent of time.

Then using the equivalent system as in Fig. 3, it may be shown that the pipe will be dynamically similar to the compressor if

$$\left(\frac{\ell}{A\rho}\right)_{pipe} = \int_{\ell}\left(\frac{d\ell}{A\rho}\right)_{compressor}$$

with the same notation as previously used.

Writing Newton's equation of motion ($F = M_a$) in the pipe

$$[p_2 - p_3]A_c = \frac{\ell A_c \rho}{g_o}\frac{du}{dt} \tag{29}$$

or putting (29) in dimensionless form

$$\frac{(p_2 - p_3)}{\frac{1}{2}\rho V_{tip}^2} = \frac{2\ell}{g_o V_{tip}^2}\cdot\frac{du}{dt} \tag{30}$$

where V_{tip} = periphery velocity of impeller

Ac = cross sectional area of pipe

Since $uAc = \dot{V}c$ (31)

where $\dot{V}c$ = rate of volume flow through compressor

then $u = \dot{V}c/Ac$

and substituting in equation (30)

$$\frac{(p_2 - p_3)}{\frac{1}{2}\rho V_{tip}^2} = \frac{2\ell}{g_o V_{tip}}\frac{d}{dt}(\dot{V}_c)$$

or $$\frac{(p_2 - p_3)}{\frac{1}{2}\rho V_{tip}^2} = \frac{2\ell}{g_o A_c V_{tip}^2} \frac{d\dot{V}_c}{dt} \tag{31}$$

Equation (31) may be written

$$\frac{(p_2 - p_3)}{\frac{1}{2}\rho V_{tip}^2} = T \frac{d}{dt}\left(\frac{\dot{V}_c}{A_c V_{tip}}\right) \tag{32}$$

where the characteristic time T of the compressor is given by

$$T = \frac{2\ell}{g_o V_{tip}} \tag{33}$$

Assuming that the process in the plenum chamber is isothermal, the following development is made (see Fig. 6).

$$V_{t_3} = V_{a_3} + V_{w_3} \tag{34}$$

where V_{t_3} = volume of plenum tank

V_{a_3} = volume of air contained in plenum tank

V_{w_3} = volume of water in plenum tank

Also $$p_3 = p_3' + \rho g h_w \tag{35}$$

where p_3' = pressure due to air contained in plenum

h_w = height of water in plenum

ρ_w = density of water

Equation (35) may be written

$$p_3 = \frac{m_a R T_3}{V_{a_3}} + \frac{\rho_w g V_{w_3}}{A_3} \tag{36}$$

where M_a = mass of air contained in plenum

T_3 = temperature in plenum

R = gas constant

A_3 = cross section area of plenum

and is as shown in Fig. 7.

Then $$\partial p_3 = -\frac{RT_3}{V_{a_3}^2} \partial V_{a_3} + \frac{\rho_w g}{A_3} \partial V_{w_3} \tag{37}$$

and noting from equation (34)

$$V_{w_3} = V_{t_3} - V_{a_3}$$

it follows that

$$\partial V_{w_3} = -\partial V_{a_3} \tag{38}$$

and substituting in equation (37)

$$\partial p_3 = \left[\frac{m_a R T_3}{(V_{t_3}-V_{w_3})^2} + \frac{\rho_w g}{A_3}\right] \partial V_{w_3} \tag{39}$$

Taking derivative of equation (39) with respect to time

$$\frac{dp_3}{dt} = \left[\frac{m_a R T_3}{(V_{t_3}-V_{w_3})^2} + \frac{\rho_w g}{A_3}\right] \frac{dV_{w_3}}{dt} \tag{40}$$

and recognizing that

$$\frac{dV_{w_3}}{dt} = \dot{V}_c - \dot{V}_o \tag{41}$$

where $\dot{V}_o$ = rate of volume flow out of orifice then equation (40) may be written

$$\frac{dp_3}{dt} = \left[\frac{m_a R T_3}{(V_{t_3}-V_{w_3})^2} + \frac{\rho_w g}{A_3}\right] \cdot \left[\dot{V}_c - \dot{V}_o\right] \tag{42}$$

Equation (42) may be made dimensionless by dividing through by $\frac{1}{2}\rho V_{tip}^2$ and rearranging as follows:

$$\frac{d}{dt}\left(\frac{p_3}{\frac{1}{2}\rho V_{tip}^2}\right) = \frac{A_c V_{tip}}{\frac{1}{2}\rho V_{tip}^2}\left[\frac{m_a R T_3}{(V_{t_3}-V_{w_3})^2} + \frac{\rho_w g}{A_3}\right] \cdot \left[\frac{\dot{V}_c}{A_c V_{tip}} - \frac{\dot{V}_o}{A_c V_{tip}}\right] \tag{43}$$

$$\frac{d}{dt}\left(\frac{p_3}{\frac{1}{2}\rho V_{tip}^2}\right) = \left[\frac{A_c m_a R T_3}{\frac{1}{2}\frac{\rho_w}{g_o} V_{tip}(V_{t_3}-V_{w_3})^2} - \frac{2A_c g}{A_3 V_{tip}}\right] \cdot \left[\frac{\dot{V}_c}{A_c V_{tip}} - \frac{\dot{V}_o}{A_c V_{tip}}\right] \tag{44}$$

Equation (44) may be written in the form

$$\frac{d}{dt}\left(\frac{p_3}{\frac{1}{2}\rho V_{tip}^2}\right) = F\left[\frac{\dot{V}_c}{A_c V_{tip}} - \frac{\dot{V}_o}{A_c V_{tip}}\right] \tag{45}$$

where the characteristic frequency of the plenum is given by

$$F = \frac{A_c m_a R T_3}{\frac{1}{2}\frac{\rho_w}{g_o} V_{tip}(V_{t_3}-V_{w_3})^2} - \frac{2A_c g}{A_3 V_{tip}} \tag{46}$$

or

$$F = \frac{A_c p_{3\,eq.}'}{\frac{1}{2}\frac{\rho_w}{g_o} V_{tip} V_{a_3}^2} - \frac{A_c}{A_3}\frac{2g}{V_{tip}} \tag{47}$$

Writing two further relationships expressing the characteristic of the compressor

$$\frac{p_2}{\frac{1}{2}\rho V_{tip}^2} = f\left(\frac{\dot{V}_c}{A_c V_{tip}}\right) \tag{48}$$

and the characteristic of the orifice

$$\frac{p_3}{\frac{1}{2}\rho V_{tip}^2} = f\left(\frac{\dot{V}_c}{A_c V_{tip}}\right) \tag{49}$$

Here once again the same assumptions are made as with the gaseous fluid, namely that for the purpose of studying stability to small disturbances, it will suffice to replace equations (48) and (49) with linear relations near the quilibrium point, with the provision that the two functions must be continuous and that their first derivatives also be continuous. Equilibrium point is defined as

$$\left(\frac{p_2}{\frac{1}{2}\rho V_{tip}^2}\right)_{eq.} = \left(\frac{p_3}{\frac{1}{2}\rho V_{tip}^2}\right)_{eq.} \tag{50}$$

and

$$\left(\frac{\dot{V}_c}{A_c V_{tip}}\right)_{eq.} = \left(\frac{\dot{V}_o}{A_c V_{tip}}\right)_{eq.} \tag{51}$$

Using these assumptions (see Fig. 8), equation (48) and (49) may be written

$$\xi_1 = X\eta_1 \tag{52}$$

$$\xi_2 = Y\eta_2 \tag{53}$$

where

$$\xi_1 = \frac{p_2}{\frac{1}{2}\rho V_{tip}^2} - \left(\frac{p_2}{\frac{1}{2}\rho V_{tip}^2}\right)_{eq} \tag{54}$$

$$\xi_2 = \frac{p_3}{\frac{1}{2}\rho V_{tip}^2} - \left(\frac{p_3}{\frac{1}{2}\rho V_{tip}^2}\right)_{eq.} \tag{55}$$

and

$$\eta_1 = \frac{\dot{V}_c}{A_c V_{tip}} - \left(\frac{\dot{V}_c}{A_c V_{tip}}\right)_{eq.} \tag{56}$$

$$\eta_2 = \frac{\dot{V}_o}{A_c V_{tip}} - \left(\frac{\dot{V}_o}{A_c V_{tip}}\right)_{eq.} \tag{57}$$

$$X = f'\left(\frac{\dot{V}_c}{A_c V_{tip}}\right) \text{ at } \left(\frac{\dot{V}_c}{A_c V_{tip}}\right)_{eq.} \tag{58}$$

$$Y = f'\left(\frac{\dot{V}_o}{A_c V_{tip}}\right) \text{ at } \left(\frac{\dot{V}_o}{A_c V_{tip}}\right)_{eq.} \tag{59}$$

As the previous work showed, X and Y are the slopes of the characteristic curves of the compressor and the orifice at the equilibrium point as shown in Fig. 8.

Substituting the new variables ξ and η in equations (45) and (32), they become

$$\xi_1 - \xi_2 = T \frac{d}{dt}(\eta_1) \tag{60}$$

$$\frac{d}{dt}(\xi_2) = F(\eta_1 - \eta_2) \tag{61}$$

and using the values of equations (52) and (53) then equations (60) and (61) may be rewritten

$$X\eta_1 - Y\eta_2 = T \frac{d}{dt}(\eta_1) \tag{62}$$

$$Y \frac{d}{dt}(\eta_2) = F(\eta_1 - \eta_2) \tag{63}$$

and a solution of the equations (62) and (63) is as before

$$\eta_1 = c_1 e^{bt}$$

$$\eta_2 = c_2 e^{bt}$$

The equations are of the same type as the gaseous fluid equation and the same condition for stability applies.

The objective of this experimental research is to construct and investigate a system which is unstable at reduced mass flow and which will therefore experience surge phenomena.

III. Summary

The water analog system was assembled as shown in Fig. 9. Impeller configurations as described in Equipment and Procedure were tested with the results described below.

No configuration tested possessed sufficiently rising pressure-flow characteristics so as to cause the water analog system to surge.

A summary of the DeLaval impeller's pressure-flow characteristics for the different configurations tested follows.

Backward Blading

The test data, Fig. 10, shows the impeller to have a rapidly falling pressure-flow characteristic with little or not possibility of instability existing. Passages of the impeller were plugged to investigate the condition whereby different type pressure-flow characteristics might exist within the separate impeller passages. The data indicates that the slope of the pressure-flow curve was not improved in so doing (see Fig. 10), but became even more stable, due to increased flow rates in the remaining passages.

It is to be concluded that the impeller rotating with backward blading has rapidly falling pressure-flow characteristics. Separate passages in this configuration did not possess pressure-flow characteristics of unlike slopes.

Forward Blading

In this configuration the impeller has a falling pressure-flow characteristic (see Fig. 11). The negative slope of the pressure-flow curve has been considerably reduced from that of the backward blading. Test data indicate separate passages to

have pressure-flow characteristics of the same slope (see Fig. 11).

It is to be concluded that the impeller rotating with forward blading has falling pressure-flow characteristics. Separate passages in this configuration did not possess pressure-flow characteristics of unlike slopes.

Forward Blading With Inducers

The impeller with inducers fitted and no passages plugged has an almost flat pressure-flow characteristic at low flow values (see Fig. 12). The inducers provided a large improvement over previous impeller configurations.

When the impeller was operated with plugged passages, the slope of the pressure-flow curve increased negatively. This again may be attributed to higher losses associated with increased flow rates of the passages in use.

The inducers improved the slope towards that of the desired pressure-flow characteristic, but not to the extent that instability was introduced.

IV. Equipment

The equipment used for the purpose of investigating compressor surge was designed to act as an hydraulic analog of an aircraft gas turbine power plant. The setup was arranged to provide a closed cycle system, with the reservoir open to the atmosphere. See Figs. 9 and 9a.

The investigation was conducted using water as the fluid, with compressibility being simulated by the air cushion provided in the plenum chamber. When operating, flow was delivered from the reservoir to a centrifugal pump; from there it was carried under pressure through the plenum chamber, through a calibrated orifice, and finally returned to the reservoir.

The reservoir consisted of a 96.2-gallon tank, 2.01 feet in diameter. Flow to the system was through a fitting two inches from the base of the container, through a gate valve, then through 4.0 feet of 2 1/2 inch pipe to the pump inlet. An orifice flange was provided near the center of this section of pipe in order to measure any reverse flow which might occur in this part of the system. The operating characteristics of the system did not, however, require an orifice plate at this position for any of the impeller configurations investigated.

The pump which was used to simulate a compressor in the system was a modified DeLaval centrifugal pump, originally rated at a head of 90 feet, delivering 179 gallons per minute at 3000 rpm. The impeller was of the double-entry type, with axial entrances. It was fully shrouded, with an outer diameter

of 7.06 inches, with the discharge passage 0.45 inches in width at the periphery. The rotor was fitted with four curved blades which in the unmodified form swept backwards at an angle of 10 degrees from the tangent line at the periphery. These blades were so shaped as to extend over an angle of 180 degrees about the rotor axis between entrance and exit. See Fig. 13.

The pump casing was of the volute type and provided no fixed blading to aid in the diffusion. The axially symmetric arrangement of rotor and seals permitted modification of the pump from the original backward swept vanes by simply reversing the shaft end-for-end. See Fig. 14.

A systematic series of modifications were made to the rotor and investigated to determine their effect upon the characteristic curve. These modifications included the design and attachment of inducers to the blades at the impeller entrance. These were cut of brass stock and formed to a compound curve providing a smooth turn of flow of nearly 180 degrees from their point of attachment at the shaft to the point at which they joined the impeller blade leading edge. See Fig. 16.

The pump was driven by a 3-horsepower, 220-volt, direct current motor, which was equipped with variable resistance in both the field and armature circuits, providing a wide range of speed control. The pump and motor were connected by a standard flexible coupling. A stroboscopic tachometer was used for the determination of motor speed, and was checked against a small hand-held friction-drive mechanical tachometer.

At the pump exit the flow was directed through 20.0 feet of 2-inch pipe which connected with the plenum chamber 1.16 feet from the pump exit. The plenum chamber consisted of a 29.8-gallon, closed steel tank, 1.0 feet in diameter. This tank was fitted with a sight glass and provided with a valve at the top which made it possible to control the height of the column of water within, hence the remaining volume of air in the tank. The valve was adapted to take a high pressure airline, so that air under pressure could be used to adjust the water level while operating.

Beyond the plenum chamber 18.84 feet of 2-inch pipe returned the flow to the reservoir, where delivery was made beneath the surface in order to avoid trapping air bubbles in the water, and to provide a closed flow of the working fluid to the same ambient conditions as at the start of the cycle. A globe valve in the return line provided an adjustable orifice for the system, and a fixed orifice with manometers was installed to meter the flow.

V. Procedure

The variables available in the test procedure were considerable in number. In the inlet system the total pressure was controlled by adjusting the head of water in the reservoir or by the position of the gate valve. At the pump, the revolutions per minute were controlled by means of the available field and armature resistance in conjunction with the use of the stroboscopic tachometer. The volume of air in the plenum chamber was controlled by adjustment of the height of the water column therein, and the rate of flow of the system was adjusted by means of the globe valve. This rate of flow in turn determined the pressure ratio across the valve, which fixed the pump exit pressure, for a given pump speed.

The procedure consisted of a systematic investigation of the characteristic curves obtained with the several impeller modifications studied. Since comparative performance curves were desired, all runs were made at the same pump speed. In addition, the plenum air volume and reservoir head were closely controlled. It was necessary to operate at a pump speed of not over 1280 rpm in order to have adequate power to be able to reach this speed at all pump loads.

Each run was made starting from a fully-opened position of the adjustable orifice (globe valve). Starting at the full-flow position allowed the system to be purged of air at the start of the run, and provided continuous purging down to shut off. From the fully-opened position the valve was closed

by increments. For each valve setting, readings were taken of p_{o_1}, the pump inlet total pressure; p_{o_2}, the pump exit total pressure; p_3', the pressure in the air chamber above the water level in the plenum chamber; h_w,,the height of the water level in the plenum chamber; and manometer readings to determine rate of flow. These were recorded (see Tables I through IX) and the results presented in the form of curves. See Figs. 10 to 12.

After reaching the shut-off position of the valve, the run was continued by opening the valve by increments to the fully-opened position. The time at shut-off was held to a minimum, for it was found that even a small leakage of air through the pump shaft packing tended to accumulate within the pump casing at the no-flow condition. By moving through shut-off with a minimum of delay, reproducible results were obtained.

In order to completely investigate the characteristics of the system and its modifications, runs were made with the rotor installed in the unmodified manner, with the blades swept backward; with the rotor reversed so that the blades swept forward; with forward swept blades and inducers added to the impeller entrance blading. For each of these blade modifications further study was made of the effect of blocking the flow in certain passages between the blades. The plugs were formed by filling the selected passages with paraffin. Runs were made in each of these configurations.

VI. Results and Discussion

In order to verify the analytical expressions indicating the stability of a compressor system which were derived in the Introduction, it was necessary to modify an existing pump in such a manner as to cause it to produce an unstable characteristic curve, i.e., one in which the pressure increases with increasing mass flow. This problem proved to be of such proportions that the major part of the experimental investigation was directed at it alone.

A study was first made of the characteristics of the unmodified pump, operating at a fixed speed. The results were plotted as a curve of $\frac{p_{o_2}}{\frac{\rho}{2g} V_{tip}^2}$ versus $\frac{Q}{A V_{tip}}$. These results served as the basic values to which all the later obtained results were compared. A stable characteristic was found for this configuration, which proceeded nearly linearly downward from a shut-off pressure equal to 93.4% of that theoretically available. Since certain leakage was unavoidable within the pump casing, from the high pressure to the low pressure side of the impeller, these results were felt to verify the accuracy of the instruments and procedures used. See Fig. 10 and Table I.

Further investigation of the characteristics of the pump with the impeller mounted with backward curved blades, but with certain individual passages filled so as to prevent flow caused the slope of the characteristic curve to become even more negative. This was felt to be caused by the higher losses associated

with the increased rate of flow necessary through the remaining active passages. In every configuration which was studied, an increase in the number of plugged passages caused a similar increase in the negative slope of the characteristic curve. See Fig. 10.

As a result of those runs made with passages plugged, it may be stated that no passage was found to be unlike the others in that it carried back flow while the remainder carried normal forward flow. Any back flow which took place was distributed equally among each of the impeller passages.

By reversing the rotor end-for-end in the pump casing, it was possible to operate the unit with forward curved blades in the impeller. The theory of centrifugal pumps predicts a rising curve of pressure versus flow for such a configuration. See development in the Appendix. The results obtained show an improvement in the slope of the characteristic curve, but not to the extent of causing it to become positive. See Fig.11. The failure of the experimental results to approach predicted values was believed due to poor matching of the blade angles at the impeller entrance to the flow direction at that station. See Fig. 17. Investigation of the variations caused by filling certain of the impeller passages so as to prevent flow therein gave results which served to confirm those previously found for the backward swept blades. An increasing number of plugged passages gave an increasingly negative slope to the characteristic curve, which was nearly linear in all cases.

In order to improve the matching of blade angle to flow direction at the impeller entrance, inducers were fitted to the impeller at the entrance. (See Fig. 16).

Results obtained with this configuration were the most satisfactory of the investigation. See Fig. 12. A very slightly rising characteristic was obtained over a limited range of flow. The slope was so nearly horizontal, however, that surge could not be forced to occur.

Again, the filling of certain passages gave further confirmation to previous conclusions as to the flow through individual passages.

A presentation of the results for the three basic configurations; backward blades, forward blades, and forward blades with impellers, is given in Figs. 10 through 12. In addition, Fig. 18 summarized the overall results by combining all curves on a single page. It may be seen that the use of forward curved blades and the incorporation of inducers caused improvements in the shape of the characteristic of the pump. Neither, however, were sufficient to produce sufficient instability as to cause the system to surge.

It may also be seen that forcing the flow through a lesser number of passages in every case caused the slope to become increasingly stable, and indicated that flow through all channels was substantially the same in nature.

VII . Conclusions

An analytical investigation of stability in an hydraulic system has been shown to reduce to expressions equivalent to those obtained for a gaseous fluid compressor system. The ability to study surge in a compressor through the use of an hydraulic analog is expected to extend the field for experimental investigation.

The limited experimental investigation performed with the hydraulic system which was built provided data only within stable operating regions. This data served to verify qualitatively centrifugal pump theory, especially with regard to the effect of the blade shape on the variation of exit pressure with flow rate.

The investigation showed that when operating within the stable range there was no indication that flow through any impeller passage was reversed or dissimilar to that through all passages.

VIII. Recommendations

The design of a new impeller is shown in Fig. 21. The incorporation of such an impeller in conjunction with a diffuser as shown in Fig. 23 is predicted to give the desired pressure flow characteristic. Insufficient time available prevented the authors from thoroughly investigating the characteristics of such a configuration in this paper. It is therefore recommended that study and tests be continued on such an impeller and diffuser.

The drive mechanism of the pump as installed provides a rather limited speed range. It is recommended that a belt pulley drive be incorporated so as to extend the operating range of the centrifugal pump. The incorporation of metering equipment to measure power supplied to the electric motor is recommended. Such an arrangement would allow an overall measurement of pump efficiency.

IX. References

1. Taylor, E. S., "The Centrifugal Supercharger", Gas Turbine Laboratory, Massachusetts Institute of Technology.

2. Stepanoff, A. J., "Centrifugal and Axial Flow Pumps", John Wiley and Sons, Inc., 1948.

3. Sheets, H. E., "The Flow Through Centrifugal Compressors and Pumps", Trans. ASME, Vol. 72, 1950, pp. 1009-1015.

4. Pearson, H. and Bowmer, T., "Surging of Axial Compressors", The Aeronautical Quarterly, November, 1949.

5. Fischer, K., "Investigation of Flow in a Centrifugal Pump", NACA TM 1089, July, 1946.

6. Bullock, R. O., Wilcox, W. W., and Moses, J. J., "Experimental and Theoretical Studies of Surging in Continuous-Flow Compressors", NACA TN 1213, March, 1947.

7. Benser, W. A. and Moses, J. J., "An Investigation of the Backflow Phenomenon in Centrifugal Superchargers", ARR E5E16a, June, 1945.

8. Brooke, G. V., "Surging of Centrifugal Superchargers", ARC R and M No. 1503, 1932.

9. Church, A. H., "Centrifugal Pumps and Blowers", John Wiley and Sons, Inc., 1944.

10. Laskin, E. B. and Kofskey, M. G., "Increase in the Stable Operating Range of a Mixed Flow Compressor by Means of a Surge Inhibitor", NACA RM E7C05a, April, 1947.

Appendix A. Instrumentation

The instrumentation used included standard type pitot tubes installed at the entrance and exit to the pump for measurement of p_{o_1} and p_{o_2}. These tubes consisted of 1/4-inch copper tubing total head pickups placed at the geometric center of flow at these stations, and positioned so that their openings faced squarely into the flow.

The measurements of p_{o_1} were made using a column of water to indicate pressure. Measurements of p_{o_2} were made with a standard bourdon tube pressure gage calibrated from 0 to 30 psi.

The pressure of the air in the upper part of the plenum chamber was measured by a standard compound bourdon tube pressure gage calibrated from minus 15 to plus 30 psi.

Flow measurements were made using a 2-inch orifice fitted into a standard orifice flange in accordance with ASME standards. The pipe ends were fitted flush with the orifice plate and pressure taps drilled through the pipe to correspond to those in the flanges. The fluid used in the associated manometer was water. Calculations relating the manometer reading to the rate of mass flow are included in the Sample Calculations.

The height of the water level in the plenum chamber was observed on an attached sight glass. Readings were taken in inches above an arbitrary zero. To refer them to the system base, which is the horizontal plane through the center of the pump inlet and exit, an additional 13.0 inches must be added.

Speed control of the motor was maintained through the use

of a General Radio Company Strobotac. Reference lines for use with this instrument were marked on the end of the motor comutator. In addition, in order to avoid the possibility of mistakenly identifying a multiple of the correct speed, a small hand-held friction-driven tachometer was used when initially getting set up for a particular set of runs.

Appendix B. The Impeller

In order to construct a hydraulic system which would surge, it was necessary that the centrifugal pump impeller possess a pressure-flow characteristic as shown in Fig. 5.

In general, it is possible for impellers to have blades of three types, namely, forward, radial, or backward-curved vanes.

Since the flow into the inlet may be considered as radial so that $V_{u_1} = 0$, the virtual head for an impeller with an infinite number of vanes may be written as:

$$H = \frac{1}{g} u_2 V_{u_2} \tag{1}$$

where u_2 = wheel tip speed

V_{u_2} = component of the absolute velocity in the direction of u_2.

Various conclusions can be drawn from equation (1). Consider the impeller rotation speed N constant, then the tip speed u_2 is a constant.

From Fig. 19 it can be seen that

$$V_{u_2} = u_2 - \frac{V_{r_2}}{\tan \beta_2} \tag{2}$$

where V_{r_2} = radial component of absolute velocity V_2

β_2 = outlet angle between u_2 and w_2.

It then follows that

$$H = \frac{1}{g} u_2 \left(u_2 - \frac{V_{r_2}}{\tan \beta_2} \right) \tag{3}$$

and

$$H = \frac{1}{g} u_2^2 \left(1 - \frac{u_2 V_{r_2}}{\tan \beta_2} \right) \tag{4}$$

From equation (4) it follows then that as the flow rate changes during constant speed operation, V_{r_2} is the only variable. The impeller outlet area is constant, hence V_{r_2} is directly proportional to the flow rate, and the head versus flow rate curve will be a straight line. Fig. 20a shows the outlet velocity diagram for an impeller having an outlet angle $\beta_2{}^\circ$ less than 90° (backward curved). It can be seen that $V_{r_2}/\tan \beta_2$ is directly proportional to V_{r_2}, and it then follows that the head must decrease with an increase in V_{r_2} or flow rate.

Fig. 20b shows the outlet diagram for a radial impeller, β_2 being 90°. For this type impeller, $V_{r_2}/\tan 90^\circ$ is equal to 0, hence the head is constant with varying V_{r_2} or flow rate.

Fig. 20c shows the velocity diagram for an outlet angle β_2 greater than 90° (forward curved). Since $\tan \beta_2$ is in this case negative, then the head must increase with V_{r_2} or flow rate. The resulting head versus flow curve is shown in Fig. 15. The DeLaval impeller provided an excellent opportunity to investigate the effect of β_2 on the pressure-flow characteristic. The impeller and shaft unit were axially symmetrical and could therefore be reversed in the pump casing simulating a change from $\beta_2 < 90^\circ$ to a condition of $\beta_2 > 90^\circ$. The results of such tests are discussed in Section VI.

When the DeLaval impeller failed to produce the desired characteristic, an investigation of the separate passages within the impeller was conducted. The purpose of such tests was to determine whether there was circulation in the impeller passages,

and whether individual passages had pressure-flow characteristics of unstable slopes. If such a situation were to exist it would be possible for reverse flow to occur in particular passages (a condition for surge) and yet have the overall pump characteristic operating on a falling pressure-flow curve. The results of such tests are as shown in Section VI.

An examination of the inlet conditions to the DeLaval impeller running with forward curved vanes revealed that poor entrance conditions existed (see Fig. 17). The actual entering absolute velocity C_1 is nearly radial, possessing only a small component in the u direction due to prerotation. The required C_1, as shown in Fig. 17, is seen to have a C_{u_1} component in excess of u_1. This represents an impossible requirement unless prerotation is supplied by a separate source. However, it is clear that the velocity triangle can be measurably improved by the addition of inducers (see Fig. 16) to supply a prerotational whirl to the fluid. The results of adding such inducers are discussed in Section VI.

The DeLaval impeller as tested in its various configurations failed to produce the desired pressure-flow characteristic. A new impeller and shaft was designed to replace the DeLaval impeller. The blade angles were maintained at $\beta = 90^\circ$ and the number of vanes was increased from four to twelve. The impeller is shown in Fig. 21. Fig. 22 as taken from Stepanoff in Ref. 2 indicates that such an impeller will produce a sheet of head H_s that is 0.84 of the maximum head H_{max}.

Appendix C. Diffuser

Investigation of the need of an externally mounted expanding section at the pump exit were made by inserting a pitot tube into the stream at various distances beyond the pump exit flange. No appreciable difference in total pressure was apparent from a station well within the pump casing to a position several feet downstream. All pressure losses apparently took place within the pump casing.

The diffuser used with the radial vaned impeller was for this reason designed as a vaned type which would fit within the casing, around the periphery of the radial vaned impeller. See Fig. 23.

Appendix D. Sample Calculations

Calculation of Flow through Standard Orifice

The flow through an orifice may be expressed in the form

$$Q = C_Q \frac{\pi d^2}{4} \left[\frac{2 \frac{\Delta p g}{\omega}}{1 - \frac{d^4}{D^4}} \right]^{1/2}$$

$$= C_q \frac{\pi}{4} d^2 \left[\frac{2 \omega_o \Delta h g}{\omega} \right]^{1/2}$$

where

Q = volume of flow in unit time

C_q = coefficient of volume, a function of Reynolds number

Δp = pressure difference across orifice

w = weight density of fluid flowing through the orifice

Δh = head on manometer measuring Δp (inches)

w_o = weight density of manometer fluid

$$Q = .63 \frac{\pi}{4} \frac{(1.5)^2}{144} \left[\frac{2 \Delta h \ 32.2}{1 - \left(\frac{1.5}{2.0}\right)^4} \right]^{1/2}$$

$$Q = 1.302 \sqrt{\Delta h} \quad ft^3/min.$$

Impeller Characteristics

p_1 = inlet pressure, lbs per square foot

v_1 = specific volume

V_1 = inlet velocity, ft per second

u_2 = impeller tip speed, ft per second

V_{t_2} = component of absolute velocity in direction of u_2

p_2 = outlet pressure, lbs per square foot

v_2 = specific volume

V_2 = outlet velocity

N = rpm = 1280

$$p_1 v_1 + \frac{V_1^2}{2g} + \frac{u_2 V_{t_2}}{g} = p_2 v_2 + \frac{V_2^2}{2g} \qquad (1)$$

$$p_2 v_2 = p_1 v_1 + \frac{V_1^2}{2g} + \frac{u_2 V_{t_2}}{g} - \frac{V_2^2}{2g} \qquad (2)$$

$$p_2 = p_1 + \frac{\rho}{2g}\left(V_1^2 - V_2\right)^2 + \frac{u_2 V_{t_2} \rho}{g} \qquad (3)$$

or $$p_2 - p_1 = \frac{\rho}{2g}\left(V_1^2 - V_2\right)^2 + \frac{u_2 V_{t_2} \rho}{g} \qquad (4)$$

For the specific system (see Fig. 19) wherein

N = 1280 rpm

r_t = radius tip impeller = 3.56 inches

D_i = diameter inlet = 2 1/2 inches

D_r = diameter outlet = 2 inches

Q = flow rate, cubic feet per sec.

V_{r_2} = radial component of V_2 to impeller, ft per sec.

w = width of outlet area at impeller periphery ft^2

W_2 = relative velocity, ft per sec.

then

$$u_2 = r\omega = \frac{3.56}{12} \times \frac{2\pi \times 1280}{60} = 39.8 \text{ ft./sec.}$$

$$V_1 = \frac{Q}{A} = \frac{Q}{\frac{\pi}{4}\frac{(2.5)}{144}^2} = 29.3\,Q \text{ ft/sec.}$$

$$V_2 = \frac{Q}{A_2} = \frac{Q}{\frac{\pi}{4}\frac{(20)}{144}^2} = 45.8\,Q \text{ ft./sec.}$$

$$V_{r_2} = \frac{Q}{\pi D_i w} = \frac{Q}{\pi \times \frac{7.125}{12} \times \frac{15}{32 \times 12}} = 13.72\,Q \text{ ft/sec.}$$

$$V_{t_2} = u_2 + W_2 \cos 10^\circ$$

$$W_2 = \frac{V_{r_2}}{\sin 10^\circ}$$

so then:

$$V_{t_2} = u_2 + \frac{V_{r_2}}{\tan 10^\circ} = u_2 + \frac{13.72Q}{.1758} = u_2 + 78.3Q$$

Substituting into equation (4)

$$p_2 - p_1 = \frac{\rho Q^2}{2g}\left(\overline{29.3}^2 - \overline{45.8}^2\right) + 39.8(78.3Q)\frac{\rho}{g} + \frac{u_2^2\rho}{g}$$

$$p_2 - p_1 = \frac{\rho}{2g}\left[(860-2100)Q^2 + 6240Q + 2u_2^2\right]$$

$$p_2 - p_1 = \frac{\rho}{2g}\left[6240Q - 1240Q^2 - 3170\right]$$

$$p_2 - p_1 = \frac{62.4}{2(32.2)}\left[6240Q - 1240Q^2 - 3170\right]$$

$$p_2 - p_1 = 6050Q - 1202Q^2 + 3070$$

Equation (5) is plotted by substituting values of Q and is shown in Fig. 24.

Q	$p_2 - p_1$ lbs/ft^2
0	3070
1	7918
2	10362
3	10402
4	8038

Appendix E

The radial impeller (see Fig. 21) was operated with and without the diffuser which is shown in Fig. 23. The curves are as shown in Fig. 25.

The preliminary tests indicate the Q-H curve at 1280 rpm to be considerably flattened. It is interesting to note that the curves are in excellent agreement with Fig. 15. The diffuser as designed shifted slightly within the compressor casing and did not operate at maximum effectiveness. The redesign of such a diffuser is recommended by the authors.

The impeller design is definitely an improvement over the DeLaval type. Investigation should be carried out at varying operating speeds in conjunction with a new diffuser design. If such investigation fails to produce the desired instability, it is recommended that the blades be replaced with forward blading maintaining the same inlet conditions as are now present.

TABLE I
EXPERIMENTAL RESULTS, UNMODIFIED ROTOR

p_{o_1}	p_{o_2}	p'_3	h_w	Δh	Q	$\frac{p_{o_2}}{\frac{1}{2}\rho V_2^2}$	$\frac{Q}{AV_2}$
.475	7.5	6.9	25.6	41.0	8.34	.715	.506
.475	7.7	6.9	25.9	37.2	7.95	.733	.482
.472	8.0	7.1	26.3	30.0	7.13	.761	.433
.468	8.0	7.1	26.5	26.9	6.75	.761	.410
.468	8.1	7.3	26.9	23.1	6.21	.771	.380
.465	8.5	7.7	27.1	15.8	5.18	.810	.314
.465	8.6	7.8	27.3	12.6	4.62	.820	.280
.465	8.7	8.0	27.5	9.4	4.00	.829	.243
.465	9.0	8.1	27.9	6.2	3.25	.856	.197
.465	9.2	8.5	28.1	2.7	2.14	.876	.130
.465	9.5	8.8	28.4	0.5	0.97	.905	.059
.465	9.8	9.1	28.5	0.0	0.0	.934	0.0
.465	9.4	8.9	28.3	1.0	1.30	.847	.079
.465	9.0	8.3	28.0	4.4	2.74	.856	.166
.465	8.8	8.1	27.6	9.2	3.95	.838	.240
.468	8.6	8.0	27.5	12.7	4.64	.820	.282
.468	8.4	8.0	27.3	15.7	5.17	.800	.313
.468	8.2	7.6	27.0	18.9	5.67	.781	.344
.472	8.1	7.5	26.8	23.5	6.32	.771	.384
.472	8.0	7.3	26.6	28.1	6.91	.761	.420
.475	7.8	7.2	26.3	32.5	7.42	.743	.450
.479	7.7	7.1	26.0	35.9	7.80	.735	.473
.479	7.5	7.0	25.8	39.6	8.20	.715	.498

TABLE II
EXPERIMENTAL RESULTS, BACKWARD CURVED BLADES,
TWO PASSAGES BLOCKED

p_{o_1}	p_{o_2}	p'_3	h_w	Δh	Q'	$\frac{p_{o_2}}{\frac{1}{2}\rho V_t^2}$	$\frac{Q}{AV_t}$
.504	2.7	2.1	20.2	28.7	6.97	.257	.422
.502	2.8	2.3	20.5	25.4	6.55	.266	.397
.502	3.3	2.8	20.7	22.7	6.20	.314	.376
.500	3.7	3.0	21.2	20.5	5.90	.352	.358
.500	3.5	2.9	21.0	17.8	5.50	.333	.334
.500	3.7	3.0	21.3	15.5	5.13	.352	.312
.500	4.1	3.2	21.9	13.6	4.80	.390	.291
.496	4.4	3.8	22.6	11.4	4.39	.419	.266
.494	5.2	4.1	23.0	9.3	3.97	.495	.241
.492	5.8	4.8	23.5	7.0	3.45	.552	.209
.489	6.2	5.2	24.0	5.4	3.01	.590	.183
.485	6.9	5.9	24.9	3.5	2.43	.657	.147
.478	8.0	7.1	26.5	0.7	1.09	.761	.066
.472	8.6	7.7	27.1	0.0	0.0	.818	0.0
.476	7.1	6.1	25.4	2.9	2.21	.675	.134
.480	6.6	5.7	24.4	5.1	2.94	.628	.178
.485	5.5	4.7	23.2	8.8	3.86	.523	.234
.492	4.6	3.8	22.5	13.1	4.72	.437	.286
.496	4.0	3.2	21.1	17.0	5.38	.381	.327
.500	3.7	3.0	20.7	19.0	5.68	.352	.345
.500	3.2	2.5	20.2	21.4	6.03	.304	.366

TABLE III
EXPERIMENTAL RESULTS, FORWARD CURVED BLADES

p_{o_1}	p_{o_2}	p_i	h_w	Δh	Q	$\frac{p_{o_2}}{\frac{1}{2}\rho V_t^2}$	$\frac{Q}{AV_t}$
.655	4.8	4.1	17.5	45.5	8.78	.457	.583
.648	4.8	4.1	17.6	39.9	8.23	.457	.500
.642	4.9	4.2	17.6	38.5	8.08	.466	.491
.647	5.1	4.3	17.8	30.5	7.19	.485	.436
.645	5.0	4.3	18.8	28.5	6.95	.476	.422
.636	5.1	4.4	18.6	24.5	6.45	.485	.391
.636	5.2	4.6	18.6	23.9	6.37	.495	.386
.642	5.2	4.7	18.9	20.7	5.93	.495	.360
.636	5.4	5.0	19.2	12.6	4.63	.514	.281
.634	5.6	5.1	19.4	8.4	3.77	.533	.229
.631	5.7	5.2	19.4	4.6	2.79	.542	.169
.631	6.0	5.4	19.9	0.0	0.0	.571	0.0
.628	5.9	5.3	20.0	0.0	0.0	.561	0.0
.628	5.6	5.0	19.4	2.7	2.14	.533	.130
.628	5.6	5.0	19.3	4.8	2.85	.533	.173
.628	5.4	5.0	19.3	8.5	3.80	.514	.231
.631	5.3	4.9	19.2	11.2	4.36	.504	.265
.634	5.2	4.8	19.1	15.2	5.07	.495	.308
.636	5.2	4.8	18.9	18.5	5.60	.495	.340
.642	5.2	4.7	18.7	22.1	6.12	.495	.372
.642	5.1	4.6	18.6	25.8	6.62	.485	.402
.645	5.0	4.5	18.3	28.7	6.98	.476	.424
.648	4.9	4.1	18.0	32.5	7.43	.466	.451

TABLE IV
EXPERIMENTAL RESULTS, FORWARD CURVED BLADES,
ONE PASSAGE BLOCKED

p_{o_1}	p_{o_2}	p'_3	h_w	Δh	Q	$\frac{p_{o_2}}{\frac{1}{2}\rho V_2^2}$	$\frac{Q}{AV_2}$
.454	1.9	1.6	14.9	14.6	4.97	.181	.302
.458	2.1	1.8	15.5	12.7	4.64	.200	.282
.458	2.4	2.0	16.0	10.4	4.20	.228	.255
.458	2.5	2.1	16.2	9.6	4.03	.238	.245
.458	2.7	2.3	16.5	7.5	3.57	.257	.217
.458	3.0	2.6	16.6	5.0	2.92	.286	.177
.458	3.3	2.8	16.9	4.1	2.64	.314	.160
.458	3.5	3.1	17.3	2.9	2.22	.333	.135
.458	3.6	3.1	17.3	1.5	1.59	.343	.096
.458	4.0	3.4	17.4	0.4	0.77	.381	.047
.458	4.5	3.8	17.5	0.0	0.0	.429	0.0
.458	4.5	3.8	17.5	0.0	0.0	.429	0.0
.458	3.8	3.2	17.5	1.3	1.48	.362	.090
.461	3.4	3.0	17.2	2.6	2.10	.324	.127
.457	3.3	2.8	16.8	5.2	2.97	.314	.180
.461	2.8	2.5	16.4	8.5	3.79	.266	.230
.461	2.1	2.0	15.6	12.8	4.66	.200	.283
.461	2.0	1.8	15.0	14.7	4.99	.190	.303

TABLE V
EXPERIMENTAL RESULTS, FORWARD CURVED VANES,
TWO PASSAGES BLOCKED

p_{o_1}	p_{o_2}	p'_3	h_w	Δh	Q	$\frac{p_{o_2}}{\frac{1}{2}\rho V_t^2}$	$\frac{Q}{AV_t}$
.483	0.9	0.3	18.4	7.4	3.54	.086	.215
.483	0.9	0.5	18.7	6.4	3.28	.086	.199
.479	1.0	0.7	18.9	5.8	3.14	.095	.191
.479	1.1	0.8	19.3	5.0	2.91	.105	.176
.475	1.3	1.0	19.8	4.1	2.64	.124	.160
.471	1.7	1.2	20.0	3.2	2.33	.162	.141
.468	1.9	1.4	20.1	2.6	2.10	.181	.127
.466	2.0	1.6	20.3	2.2	1.93	.190	.117
.464	2.3	1.9	20.7	1.5	1.59	.219	.097
.457	2.8	2.2	21.1	0.8	1.16	.266	.070
.453	3.3	2.7	21.9	0.3	0.71	.314	.043
.449	4.0	3.1	22.5	0.0	0.0	.381	0.0
.449	4.0	3.1	22.5	0.0	0.0	.381	0.0
.461	2.8	2.2	21.1	0.9	1.23	.266	.075
.466	2.5	2.0	20.5	2.0	1.84	.238	.112
.468	2.0	1.7	20.1	3.15	2.32	.190	.141
.470	1.6	1.2	19.8	4.4	2.73	.152	.166
.475	1.2	1.0	19.1	5.5	3.05	.114	.185
.477	1.1	0.8	18.6	6.7	3.37	.105	.204
.479	1.0	0.3	18.3	7.6	3.59	.095	.218

TABLE VI
EXPERIMENTAL RESULTS, FORWARD CURVED BLADES,
INDUCERS ADDED

p_{o_1}	p_{o_2}	p'_3	h_w	Δh	Q	$\frac{p_{o_2}}{\frac{1}{2}\rho V_2^2}$	$\frac{Q}{AV_2}$
.493	4.6	3.9	19.6	0.0	0.0	.438	0.0
.486	4.7	3.9	19.7	0.8	1.16	.448	.070
.479	4.8	3.9	19.9	2.2	1.93	.457	.117
.475	5.0	4.2	20.1	3.7	2.51	.476	.152
.471	5.0	4.1	20.1	4.7	2.82	.476	.171
.465	4.9	4.0	19.9	6.6	3.34	.466	.203
.454	4.5	3.9	19.5	9.5	4.01	.428	.244
.450	4.0	3.2	18.6	13.1	4.71	.381	.286
.443	3.5	3.0	18.1	16.5	5.30	.333	.322
.418	3.9	3.0	18.3	23.0	6.25	.371	.379
.490	5.1	4.3	19.3	0.0	0.0	.485	0.0
.490	5.1	4.2	19.2	1.0	1.30	.485	.079
.486	5.1	4.2	19.2	3.3	2.37	.485	.144
.479	5.1	4.2	19.2	5.9	3.16	.485	.192
.471	4.5	4.0	18.9	7.8	3.64	.428	.221
.468	4.3	3.6	18.1	10.1	4.14	.409	.251
.461	3.8	3.2	17.3	13.1	4.71	.362	.286
.450	3.3	2.9	16.9	17.2	5.40	.314	.328
.432	3.2	2.8	16.7	22.4	6.17	.305	.374
.414	3.2	2.8	16.7	26.0	6.64	.305	.403
.403	3.2	2.8	16.7	28.9	7.00	.305	.425
.385	3.3	2.8	16.8	31.4	7.30	.314	.443

TABLE VI
EXPERIMENTAL RESULTS, FORWARD CURVED BLADES,
INDUCERS ADDED

p_{o_1}	p_{o_2}	p'_3	h_w	Δh	Q	$\frac{p_{o_2}}{\frac{1}{2}\rho V_t^2}$	$\frac{Q}{AV_t}$
.410	3.8	3.0	18.0	25.6	6.60	.362	.400
.426	3.5	2.9	18.0	20.1	5.84	.333	.354
.450	4.0	3.2	18.5	14.1	4.89	.381	.397
.462	4.4	3.7	19.0	11.5	4.41	.419	.268
.468	4.7	3.9	19.5	7.9	3.66	.447	.222
.475	4.9	4.0	19.8	5.5	3.05	.466	.185
.483	4.9	4.1	20.0	4.0	2.60	.466	.158
.490	5.0	4.1	20.1	2.2	1.93	.476	.117
.490	5.0	4.1	20.0	0.7	1.17	.476	.071
.490	5.0	4.1	20.1	0.0	0.0	.476	0.0
.490	4.9	4.1	20.0	0.0	0.0	.466	0.0
.490	5.0	4.1	19.9	0.9	1.23	.476	.075
.490	5.0	4.1	19.8	2.2	1.93	.476	.117
.486	4.9	4.1	19.7	3.8	2.54	.466	.154
.475	4.7	4.0	19.6	6.3	3.27	.447	.198
.468	4.5	3.9	19.2	9.4	3.99	.429	.242
.459	4.2	3.6	18.6	14.0	4.86	.400	.295
.443	3.6	3.0	18.0	19.3	5.72	.343	.347
.407	3.7	3.0	17.9	27.0	6.76	.352	.410

TABLE VII
EXPERIMENTAL RESULTS, FORWARD CURVED BLADES,
INDUCERS ADDED, ONE PASSAGE
BLOCKED

p_{o1}	p_{o2}	p'_3	h_w	Δh	Q	$\frac{p_{o2}}{\frac{1}{2}\rho V_t^2}$	$\frac{Q}{AV_t}$
.450	2.2	1.5	21.6	20.4	5.88	.209	.357
.450	2.2	1.5	21.6	18.7	5.63	.209	.342
.459	2.3	1.6	21.7	15.5	5.14	.219	.312
.461	2.4	1.8	21.9	12.6	4.80	.228	.291
.468	2.4	1.9	22.0	10.0	4.12	.228	.250
.471	2.5	2.0	22.0	7.8	3.64	.238	.221
.479	2.5	2.0	22.6	6.0	3.19	.238	.194
.479	2.6	2.0	22.6	4.4	2.73	.247	.166
.483	2.9	2.2	23.0	3.4	2.40	.276	.146
.483	3.2	2.4	23.0	2.1	1.89	.304	.115
.483	3.5	2.6	23.3	0.9	1.23	.333	.075
.483	3.7	2.9	23.5	0.0	0.0	.352	0.0
.483	3.7	2.9	23.5	0.0	0.0	.352	0.0
.483	3.5	2.8	23.4	1.0	1.30	.333	.079
.479	3.4	2.8	23.2	2.0	1.84	.324	.112
.475	3.2	2.5	23.0	3.5	2.44	.305	.148
.471	3.0	2.3	22.1	5.2	2.97	.286	.180
.468	2.5	1.9	22.0	7.2	3.50	.238	.212
.468	2.3	1.8	21.9	11.0	4.32	.219	.262
.459	2.3	1.8	21.8	13.9	4.86	.219	.295
.454	2.2	1.7	21.8	17.2	5.40	.209	.328
.443	2.2	1.6	21.6	20.9	5.95	.209	.361

TABLE VIII
EXPERIMENTAL RESULTS, FORWARD CURVED BLADES,
TWO PASSAGES BLOCKED, INDUCERS ADDED

p_{o_1}	p_{o_2}	p'_3	h_w	Δh	Q	$\frac{p_{o_2}}{\frac{1}{2}\rho V_t^2}$	$\frac{Q}{AV_t}$
.369	1.0	0.1	20.5	10.9	4.30	.095	.261
.365	1.0	0.1	20.8	10.3	4.17	.095	.253
.361	1.1	0.2	21.0	9.2	3.95	.105	.240
.361	1.3	0.5	21.2	7.4	3.54	.124	.215
.361	1.4	0.8	21.4	6.0	3.19	.133	.194
.361	1.5	0.9	21.6	5.0	2.91	.143	.177
.361	1.8	1.1	22.2	3.7	2.50	.171	.152
.361	2.2	1.5	22.6	2.0	1.84	.210	.112
.361	2.4	1.8	23.0	1.3	1.49	.228	.090
.361	2.6	1.9	23.0	0.4	0.82	.248	.050
.361	2.7	2.0	23.1	0.0	0.0	.257	0.0
.361	2.7	2.0	23.1	0.0	0.0	.257	0.0
.361	2.5	1.9	22.9	0.7	1.09	.238	.066
.361	2.4	1.8	22.9	1.4	1.54	.228	.094
.361	2.3	1.7	22.8	2.2	1.93	.219	.117
.361	2.1	1.4	22.5	3.6	2.47	.200	.150
.361	1.8	1.2	22.0	4.8	2.85	.171	.173
.369	1.4	0.9	21.4	5.7	3.11	.133	.189
.369	1.2	0.7	21.0	6.8	3.40	.114	.206
.369	1.1	0.6	21.0	9.2	3.95	.105	.240
.365	1.0	0.5	20.9	10.4	4.20	.095	.255
.367	1.0	0.5	20.8	11.1	4.34	.095	.263

TABLE IX
EXPERIMENTAL RESULTS, FORWARD CURVED BLADES,
THREE PASSAGES BLOCKED, INDUCERS ADDED

p_{o_1}	p_{o_2}	p'_3	h_w	Δh	Q	$\frac{p_w}{\frac{1}{2}\rho V_t^2}$	$\frac{Q}{AV_t}$
.490	0.1	0^+	18.2	2.8	2.18	.009	.132
.492	0.1	0^+	18.5	2.5	2.06	.009	.125
.486	0.1	0.1	18.9	2.2	1.93	.009	.117
.486	0.2	0.1	19.3	1.6	1.65	.019	.100
.486	0.8	0.2	19.7	1.2	1.43	.076	.087
.486	1.0	0.3	20.1	1.1	1.36	.095	.083
.486	1.1	0.5	20.3	0.8	1.16	.105	.070
.486	1.3	0.7	20.6	0.5	0.92	.124	.056
.486	1.5	1.0	20.8	0.2	0.58	.143	.035
.483	2.0	1.3	21.0	0.0	0.0	.190	0.0
.483	2.0	1.3	21.0	0.0	0.0	.190	0.0
.490	1.6	1.2	20.7	0.2	0.58	.152	.035
.486	1.7	1.2	20.8	0.3	0.71	.162	.043
.486	1.6	1.1	20.8	0.5	0.92	.152	.056
.486	1.4	1.0	20.5	0.8	1.16	.133	.070
.486	1.3	0.9	20.2	1.1	1.36	.124	.083
.486	1.0	0.3	19.5	1.6	1.65	.095	.100
.486	0.5	0.1	19.0	1.9	1.79	.047	.109
.486	0.1	0^+	18.5	2.4	2.02	.009	.123
.486	0^+	0^+	18.3	2.8	2.18	0^+	.132

TABLE X

EXPERIMENTAL RESULTS, RADIAL VANED IMPELLER

p_{o1}	p_{o2}	p'_3	h_w	Δh	Q	$\frac{p_{o2}-p_{o1}}{\frac{1}{2}\rho V_t^2}$	$\frac{Q}{AV_t}$
.285	10.5	9.4	28.4	13.0	4.69	.971	.285
.289	10.4	9.5	28.4	9.9	4.10	.964	.249
.292	10.5	9.6	28.5	6.5	3.32	.971	.202
.296	10.7	9.8	28.5	3.8	2.54	.990	.154
.300	10.8	9.8	28.5	2.1	1.89	1.000	.115
.303	10.9	10.0	28.6	0.7	1.09	1.010	.065
.307	11.0	10.1	28.7	0.0	0.0	1.020	0.0
.303	10.8	9.9	28.6	1.0	1.30	1.000	.079
.300	10.6	9.8	28.5	3.9	2.57	.980	.156
.296	10.5	9.7	28.5	7.1	3.47	.970	.211
.285	10.4	9.5	28.4	12.7	4.64	.961	.269
.271	10.4	9.3	28.2	17.0	5.37	.965	.326

TABLE XI

EXPERIMENTAL RESULTS, RADIAL VANED IMPELLER PLUS DIFFUSER

p_{o1}	p_{o2}	p'_3	h_w	Δh	Q	$\frac{p_{o2}-p_{o1}}{\frac{1}{2}\rho V_t^2}$	$\frac{Q}{AV_t}$
.426	10.1	9.5	18.7	27.5	6.76	.920	.410
.426	10.2	9.8	18.8	20.1	5.85	.930	.355
.430	10.2	9.9	18.8	16.3	5.26	.930	.319
.439	10.2	9.9	18.9	14.0	4.87	.929	.295
.437	10.3	9.9	19.0	11.7	4.46	.940	.271
.439	10.2	9.9	19.0	9.2	3.96	.929	.240
.441	10.3	9.9	19.1	7.4	3.54	.940	.215
.443	10.4	10.0	19.2	5.6	3.08	.949	.187
.448	10.4	10.1	19.2	4.1	2.64	.948	.160
.448	10.5	10.1	19.4	2.6	2.10	.957	.127
.450	10.6	10.2	19.5	1.2	1.43	.966	.086
.450	10.7	10.3	19.6	0.3	0.71	.976	.043
.452	10.9	10.4	19.8	0.0	0.0	.995	0.0
.450	10.5	10.2	19.5	1.6	1.65	.957	.100
.450	10.4	10.1	19.3	3.6	2.47	.948	.150
.448	10.3	10.1	19.2	5.3	3.00	.939	.182
.448	10.3	10.1	19.1	7.1	3.47	.939	.211
.441	10.2	10.0	19.0	10.0	4.12	.929	.250
.434	10.3	10.0	19.0	13.3	4.75	.941	.288
.423	10.2	9.8	18.8	18.8	5.65	.931	.343
.412	10.1	9.5	18.6	24.6	6.46	.923	.392

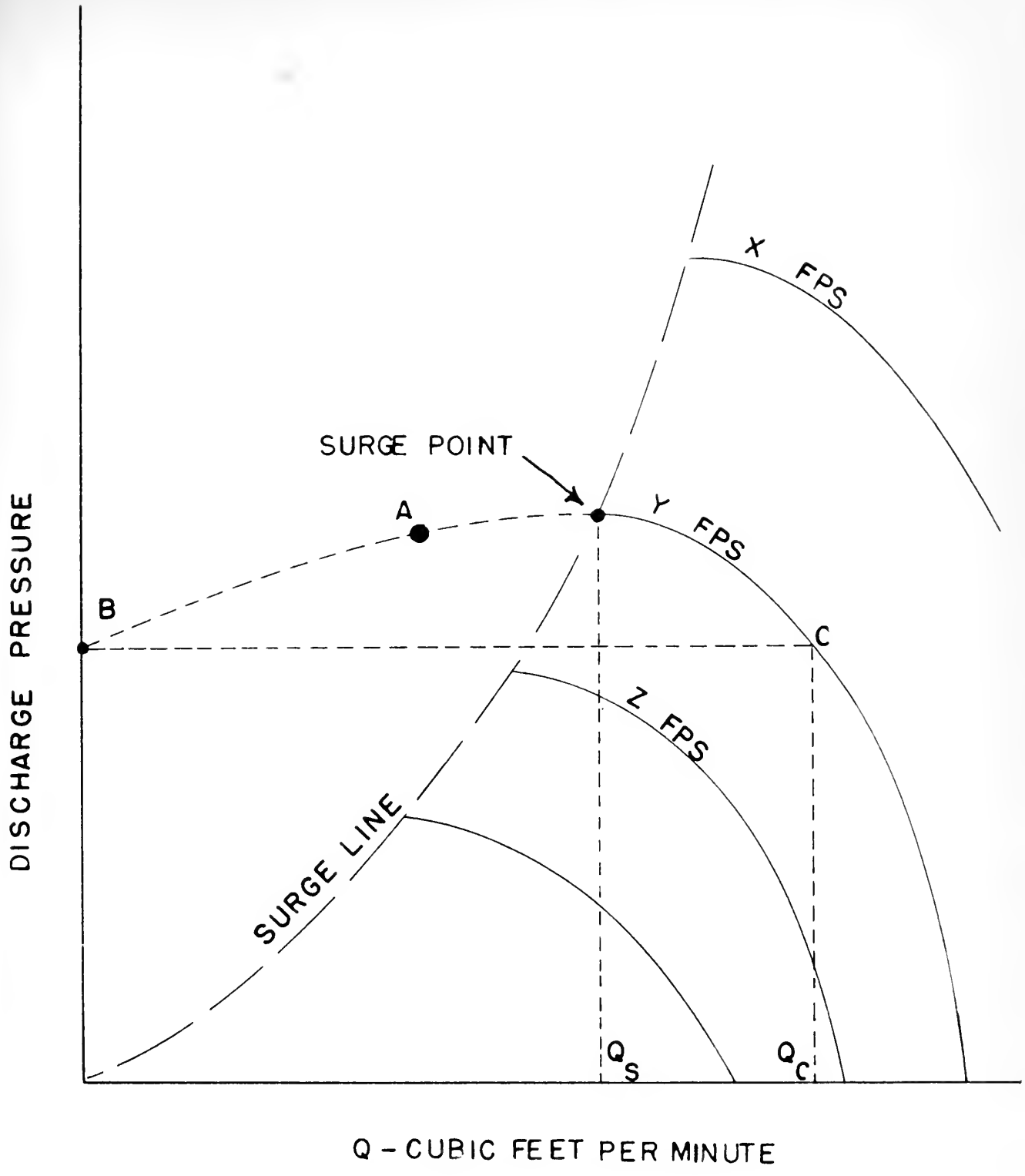

FIG. 1 PERFORMANCE CURVE FOR A TYPICAL CENTRIFUGAL COMPRESSOR

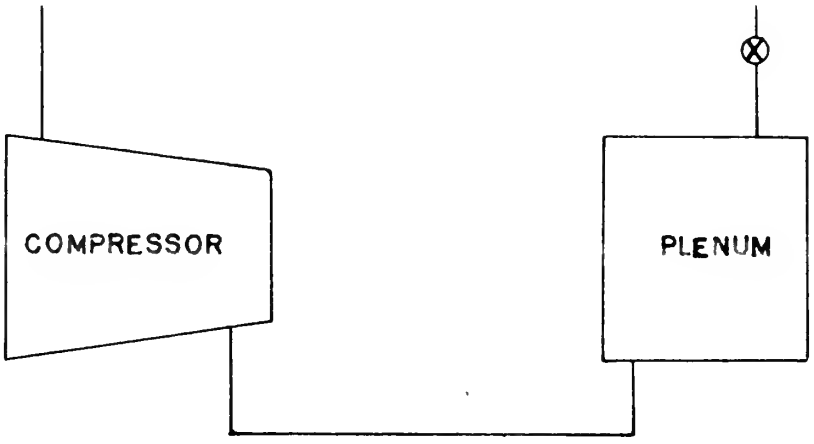

FIG. 2 DIAGRAMMATIC COMPRESSOR SET-UP

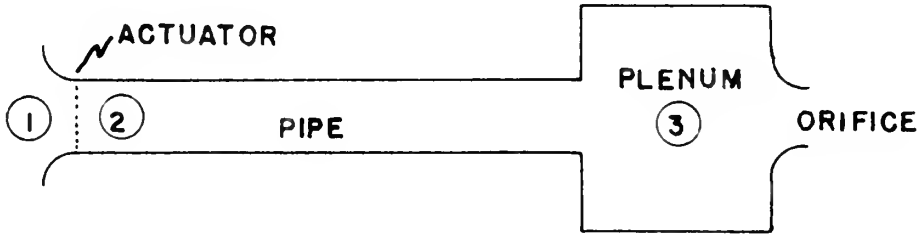

FIG. 3 ANALOGUE OF COMPRESSOR TEST SET-UP

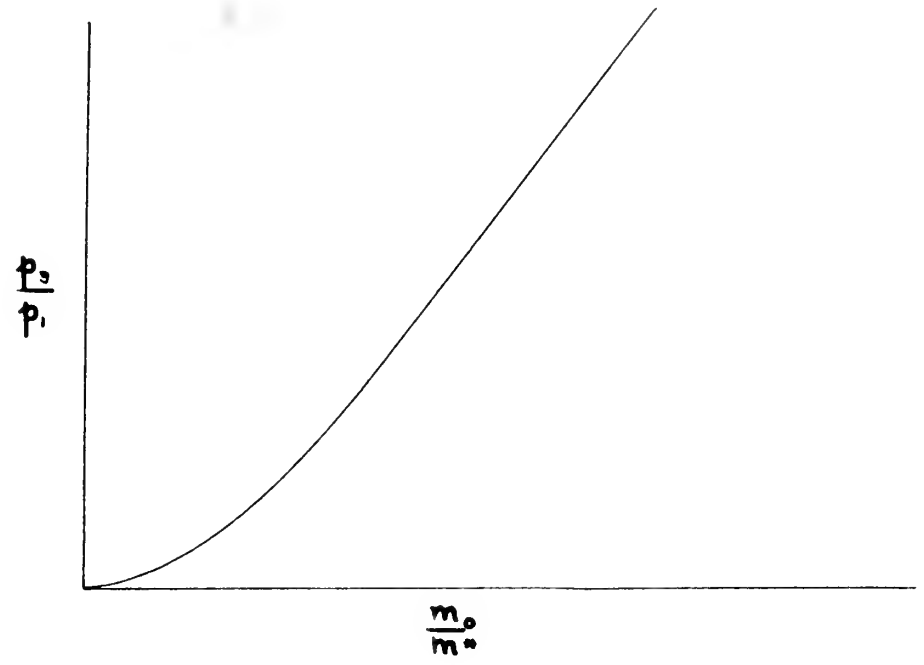

FIG. 4 ORIFICE CHARACTERISTICS

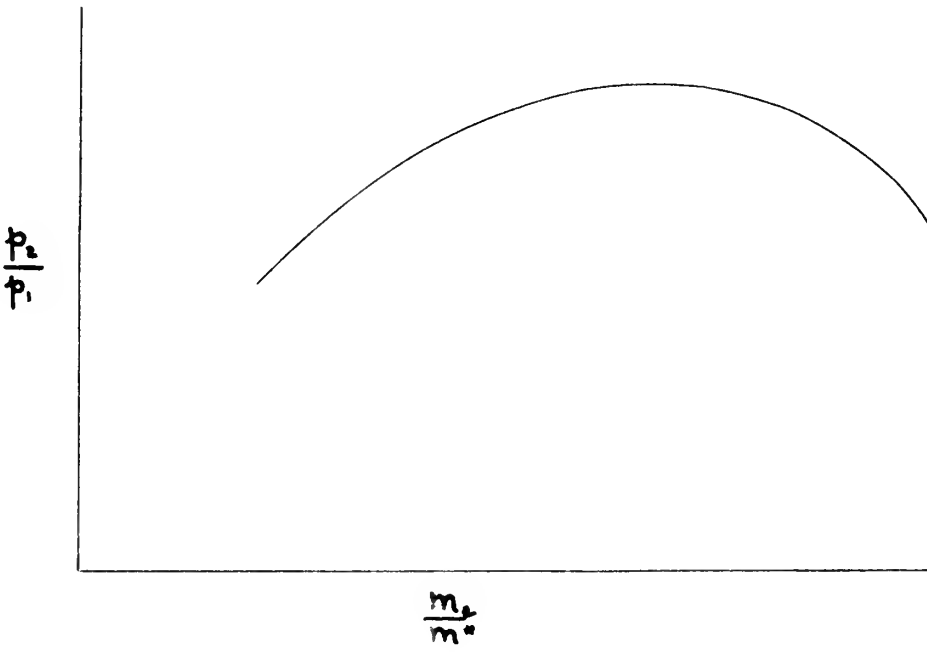

FIG. 5 STATIC COMPRESSOR CHARACTERISTICS

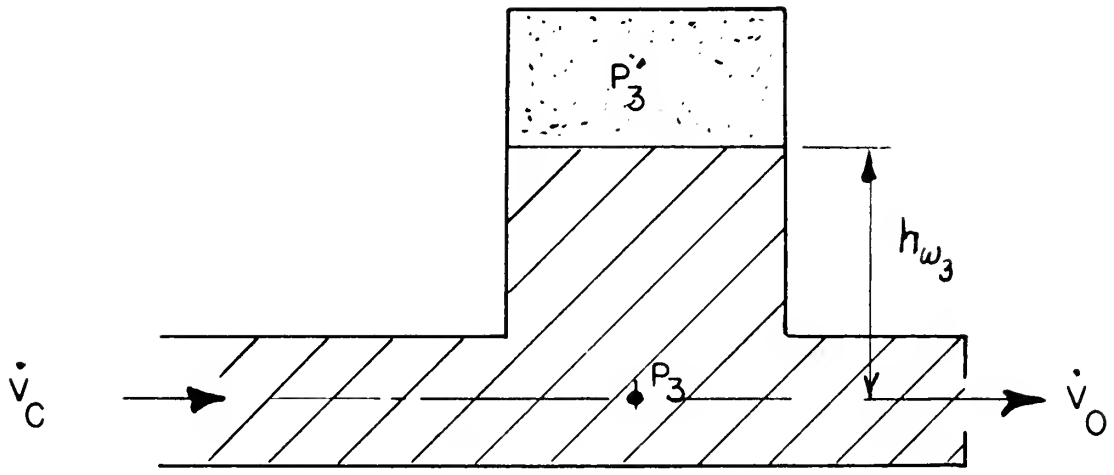

FIG. 6 HYDRAULIC ANALOGUE

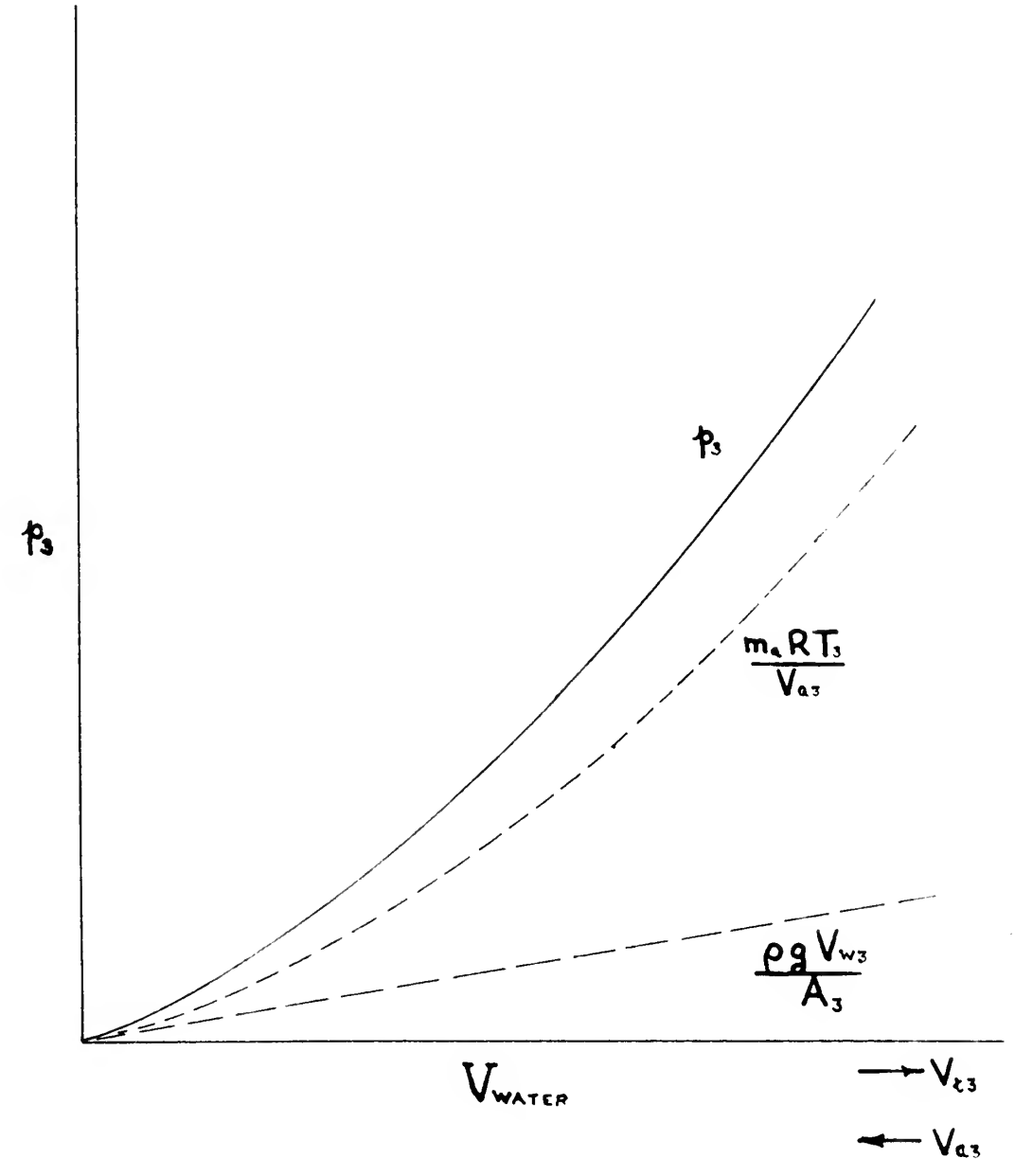

FIG. 7

$$p_3 = \frac{m_a R T_3}{V_{a3}} + \frac{\rho g V_{w3}}{A_3}$$

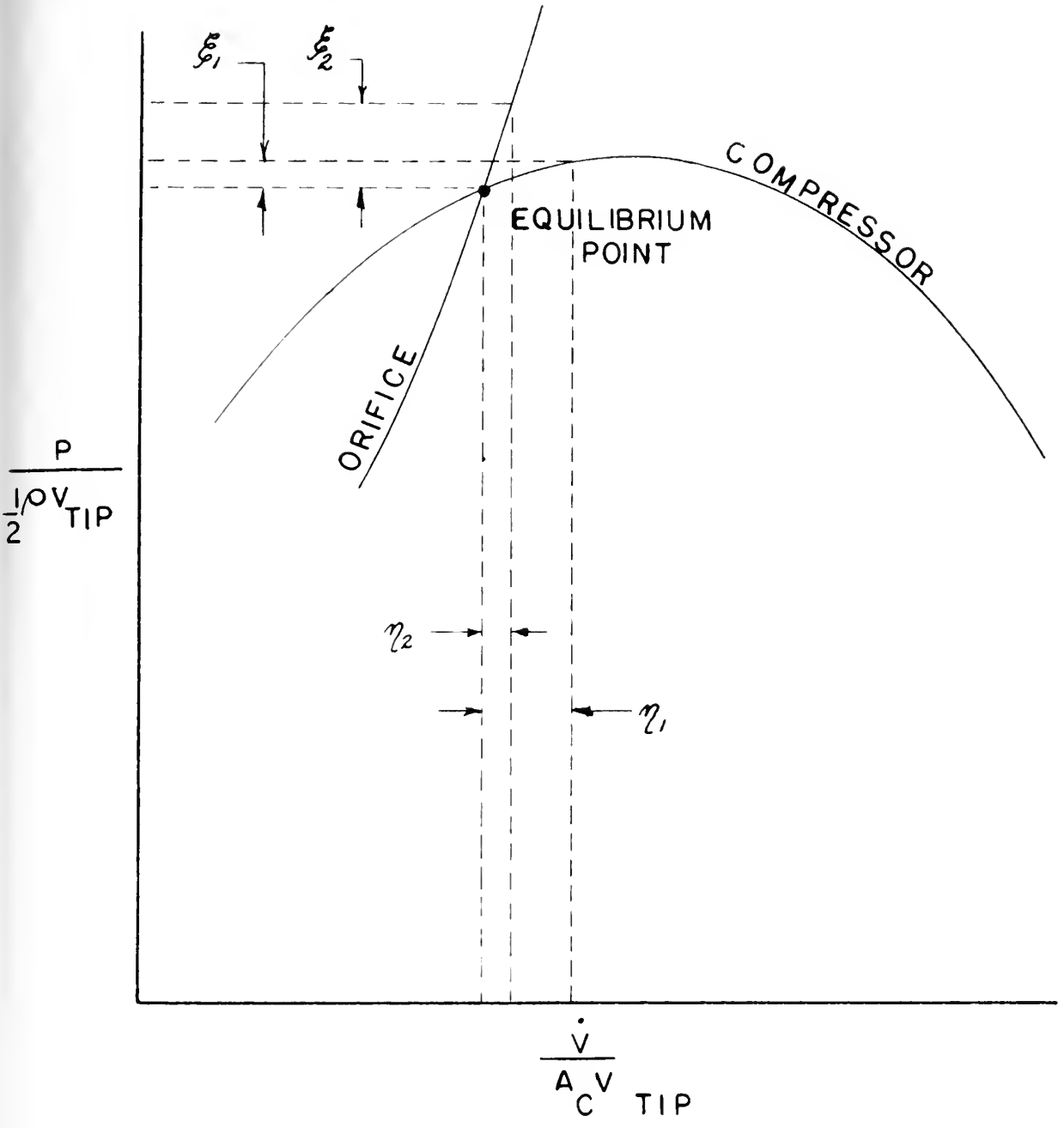

FIG. 8 LINEARIZATION NEAR EQUILIBRIUM POINT

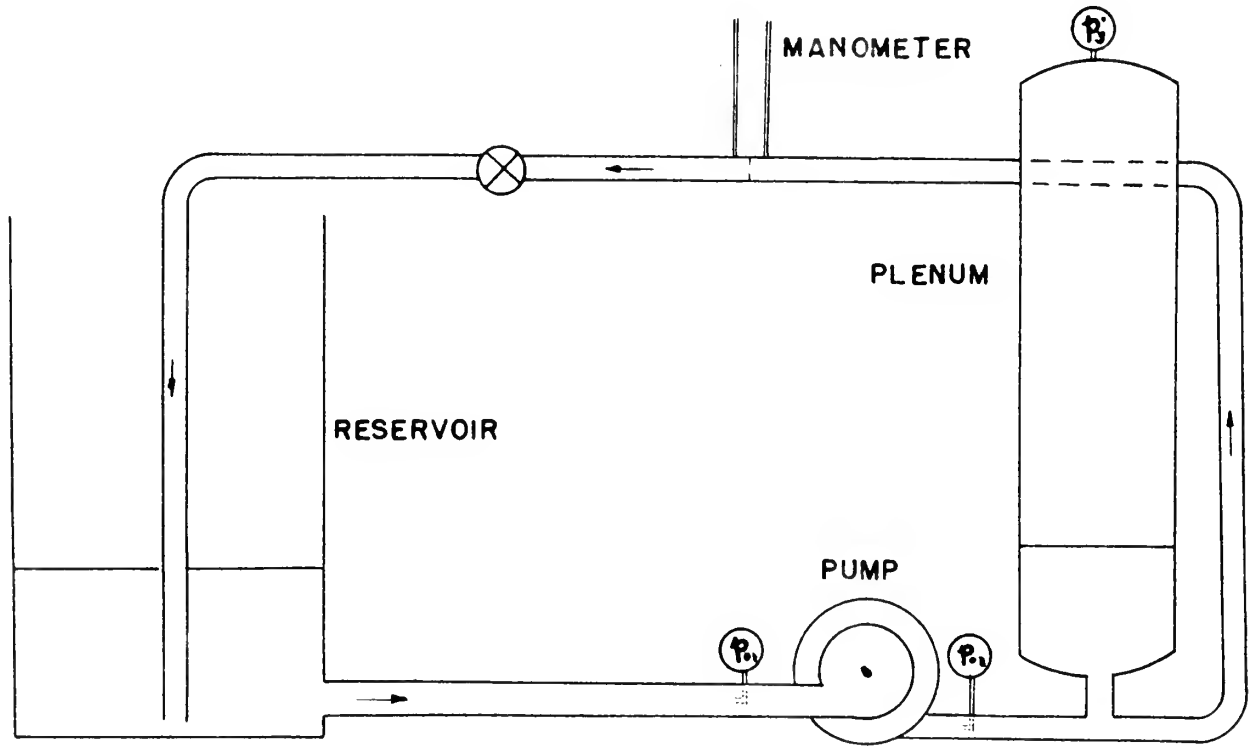

FIG. 9 SCHEMATIC EXPERIMENTAL TEST SET-UP

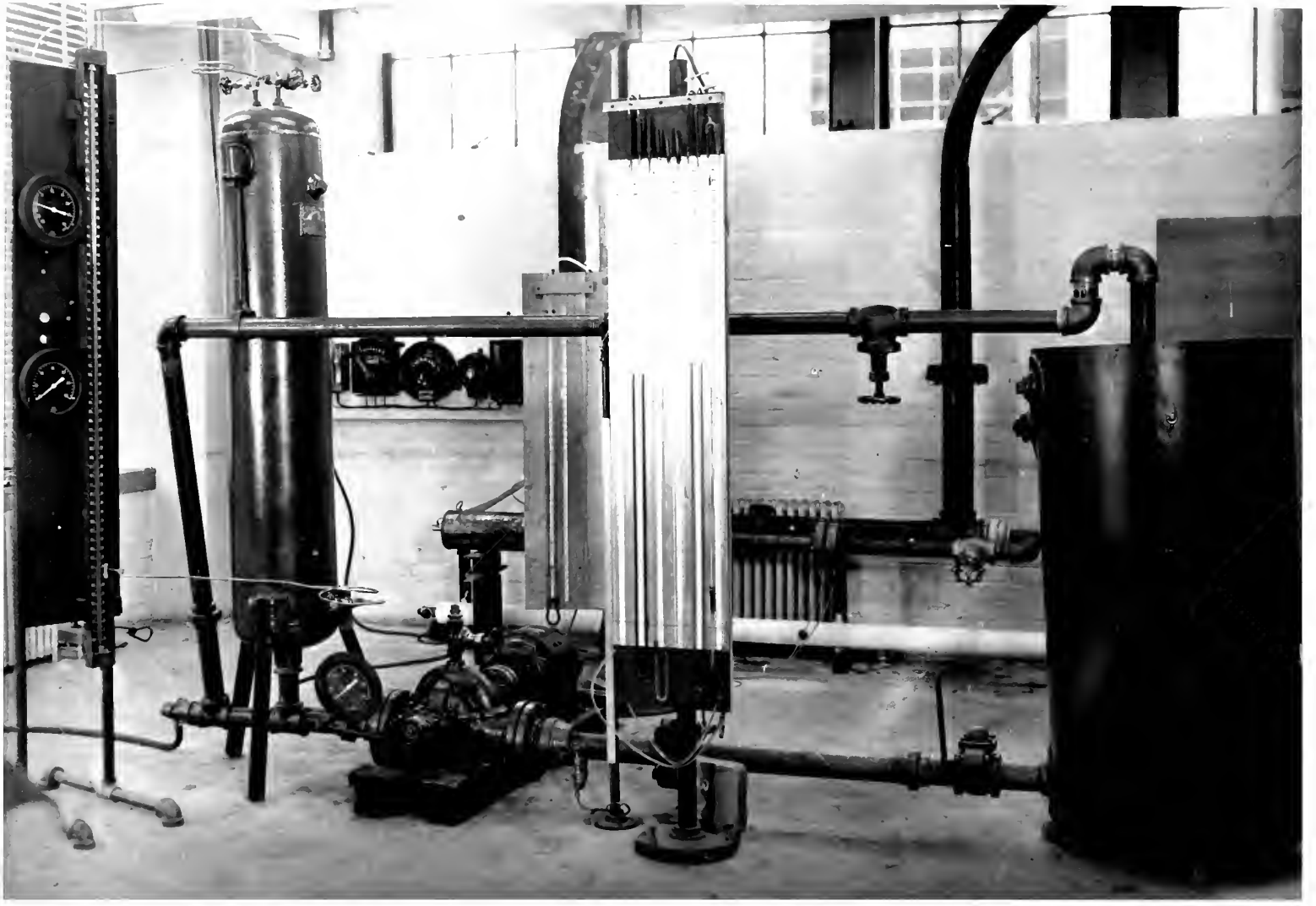

FIG. 9-a VIEW OF EXPERIMENTAL TEST SET-UP

FIG. 10

EXPERIMENTAL RESULTS,

BACKWARD CURVED BLADES

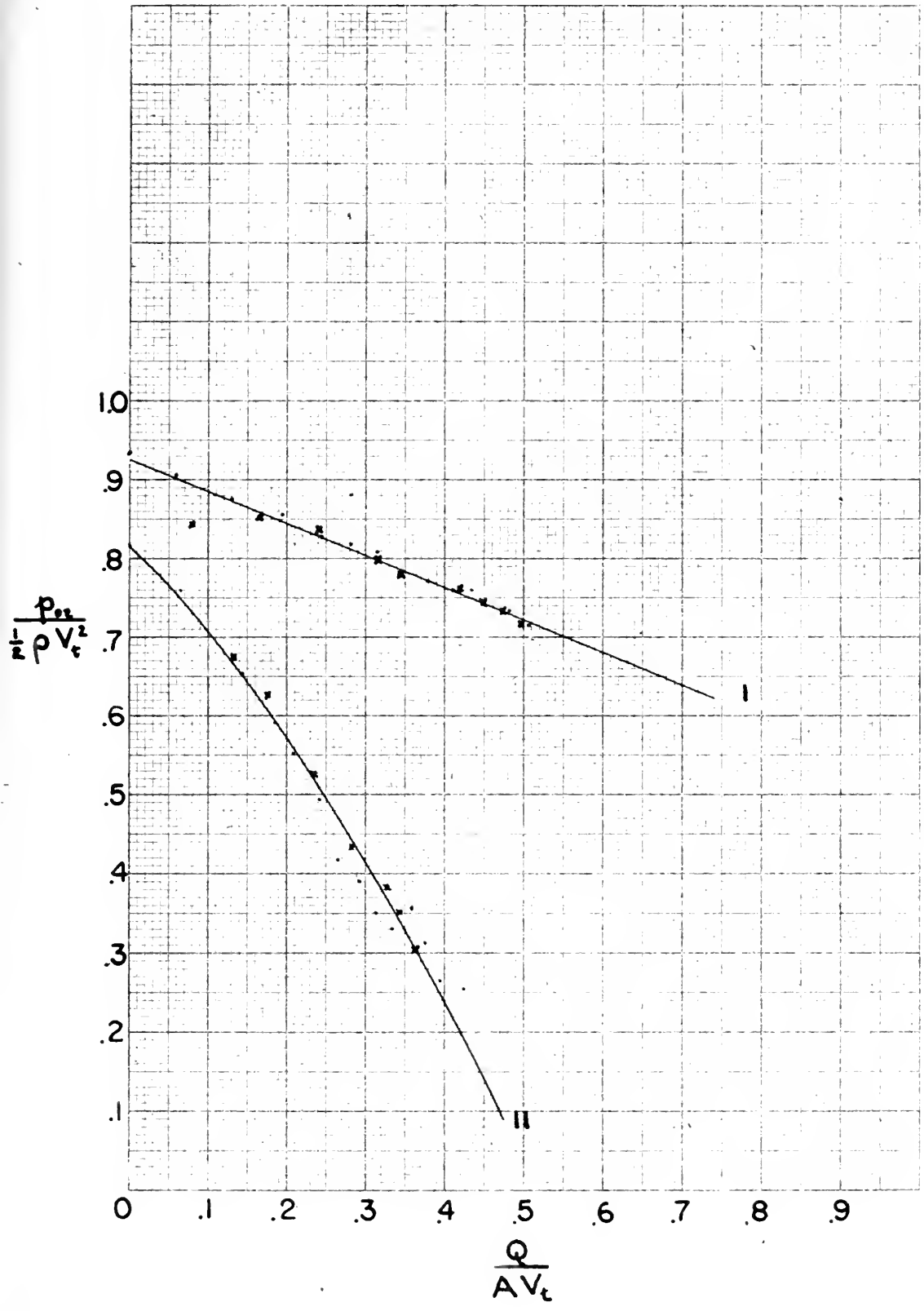

FIG. II

EXPERIMENTAL RESULTS,

FORWARD CURVED BLADES

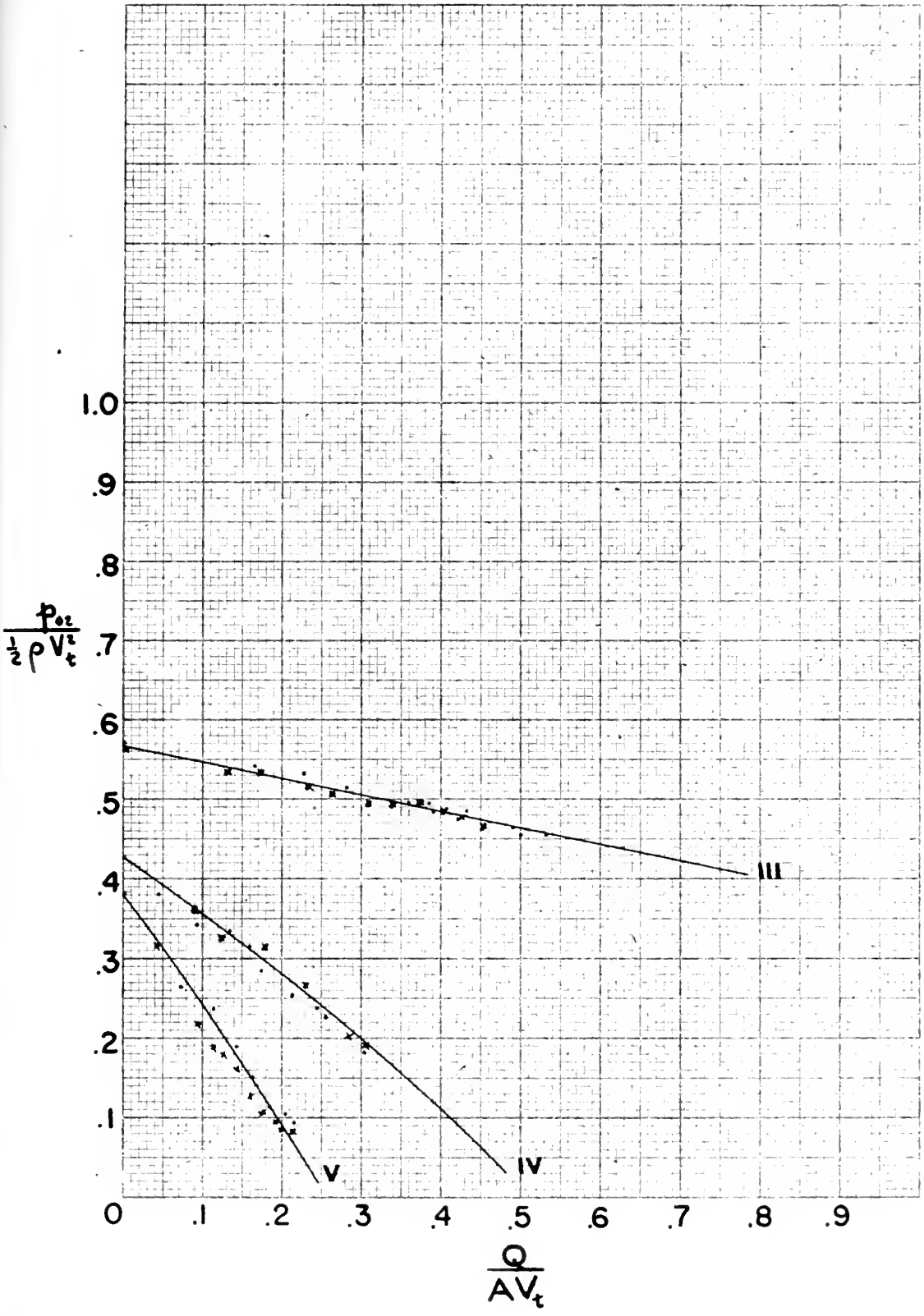

FIG. 12
EXPERIMENTAL RESULTS,
FORWARD CURVED BLADES AND INDUCERS

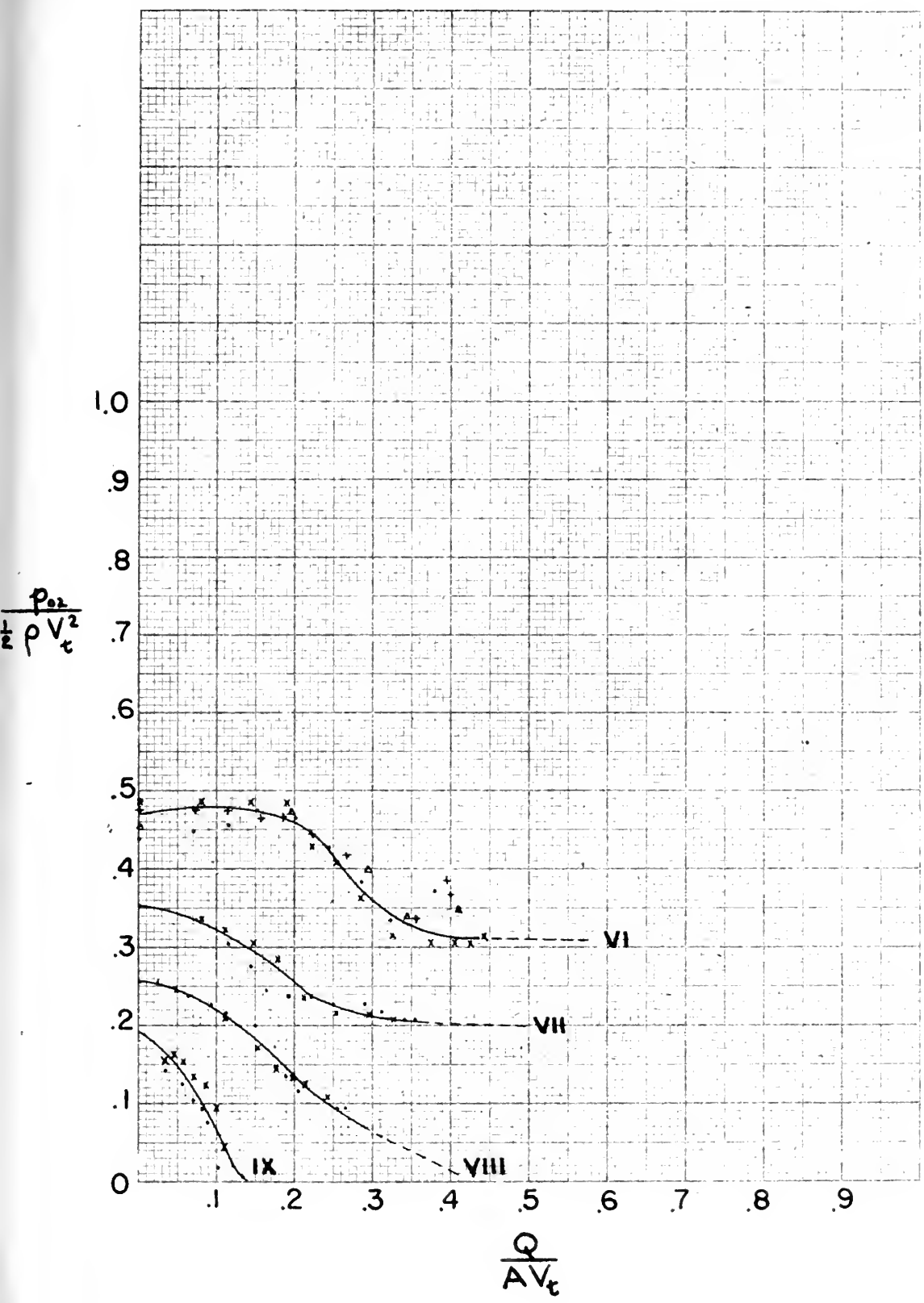

FIG. 13 VIEW OF IMPELLER

FIG. 14 VIEW OF OPENED CASING AND IMPELLER

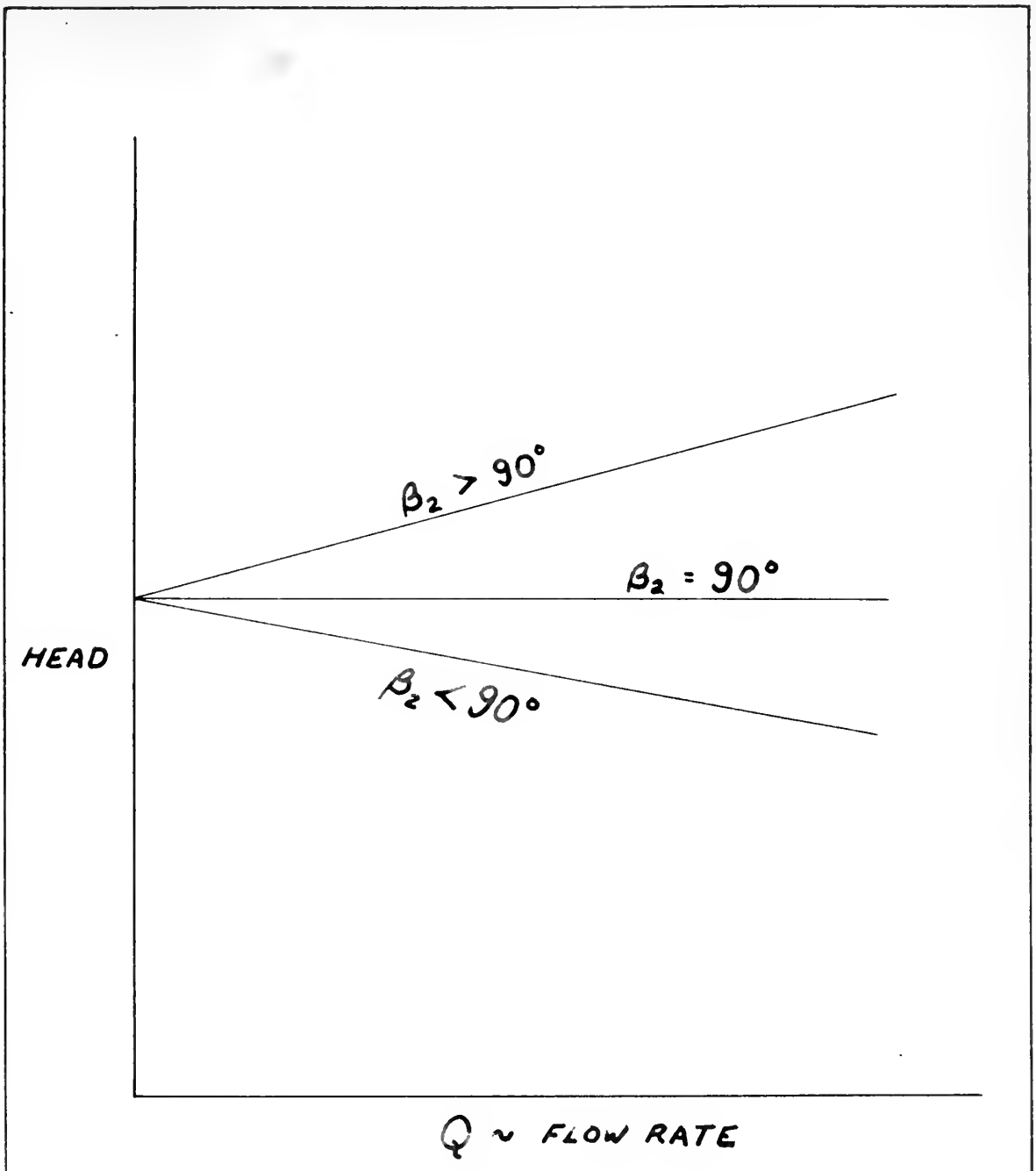

FIG. 15 HEAD CAPACITY CURVES FOR VARIOUS OUTLET ANGLES β

FIG. 16 VIEW OF IMPELLER WITH INDUCERS ATTACHED

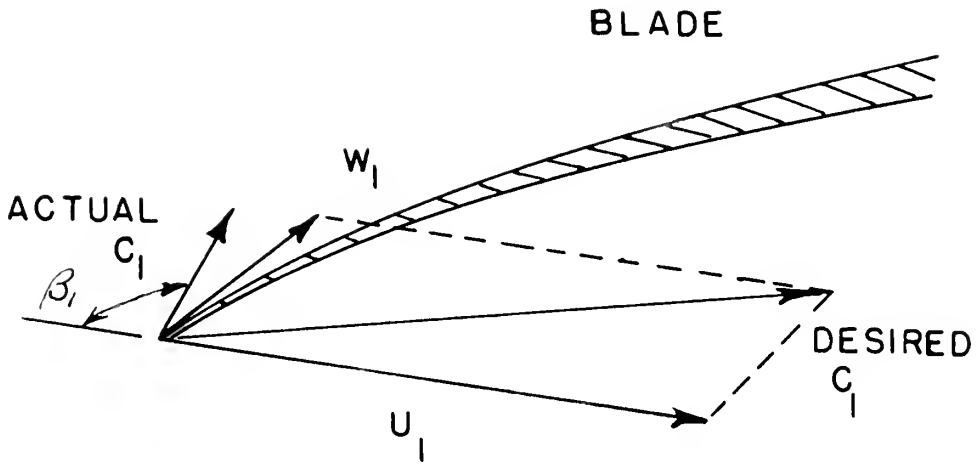

FIG. 17 ENTRANCE VELOCITY DIAGRAM TO DELAVAL IMPELLER

FIG. 18
SUMMARY OF EXPERIMENTAL RESULTS

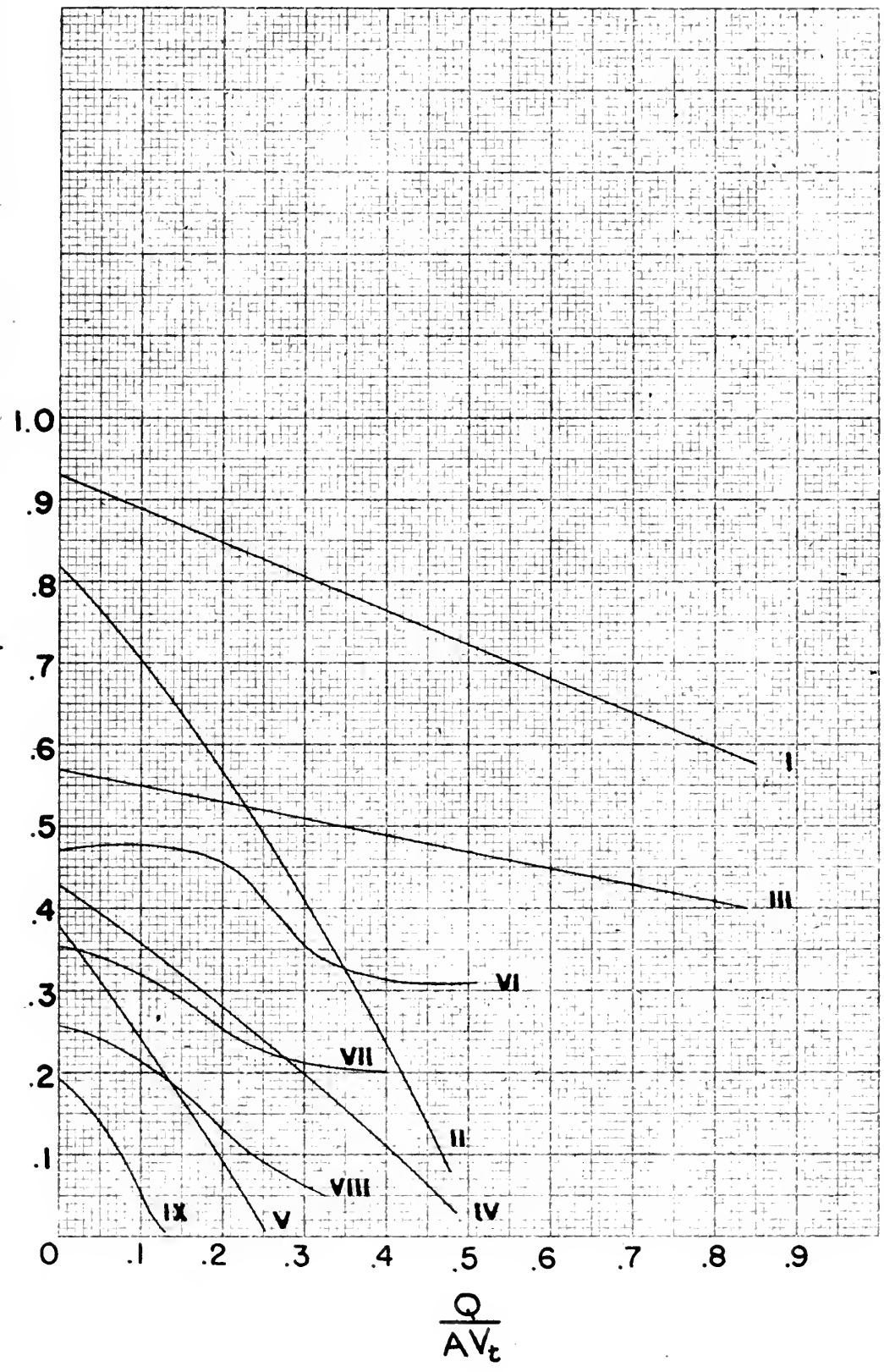

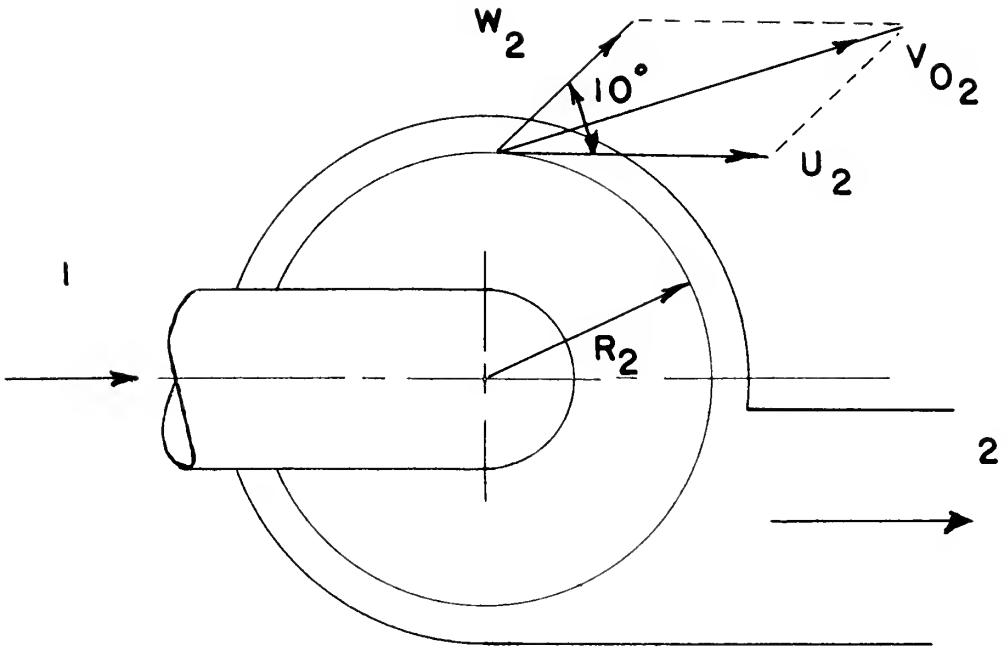

FIG. 19 CENTRIFUGAL PUMP CHARACTERISTICS

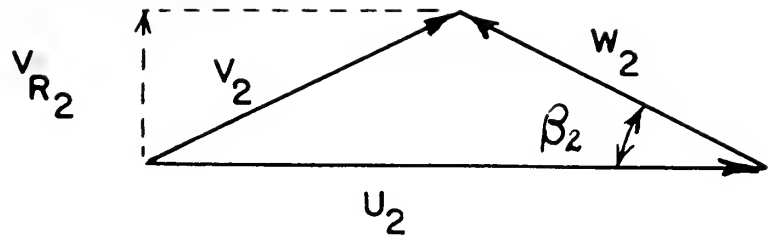

FIG. 20A OUTLET VELOCITY DIAGRAM $\beta_2 < 90^\circ$

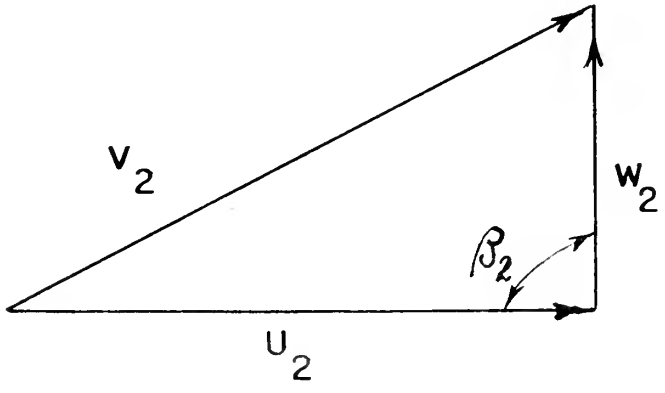

FIG. 20B OUTLET VELOCITY DIAGRAM $\beta_2 = 90^\circ$

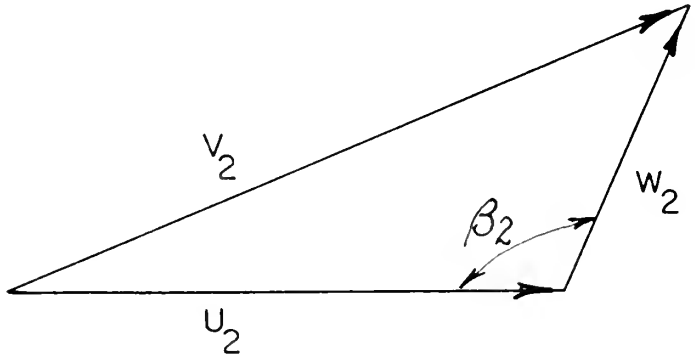

FIG. 20C OUTLET VELOCITY DIAGRAM $\beta_2 > 90^\circ$

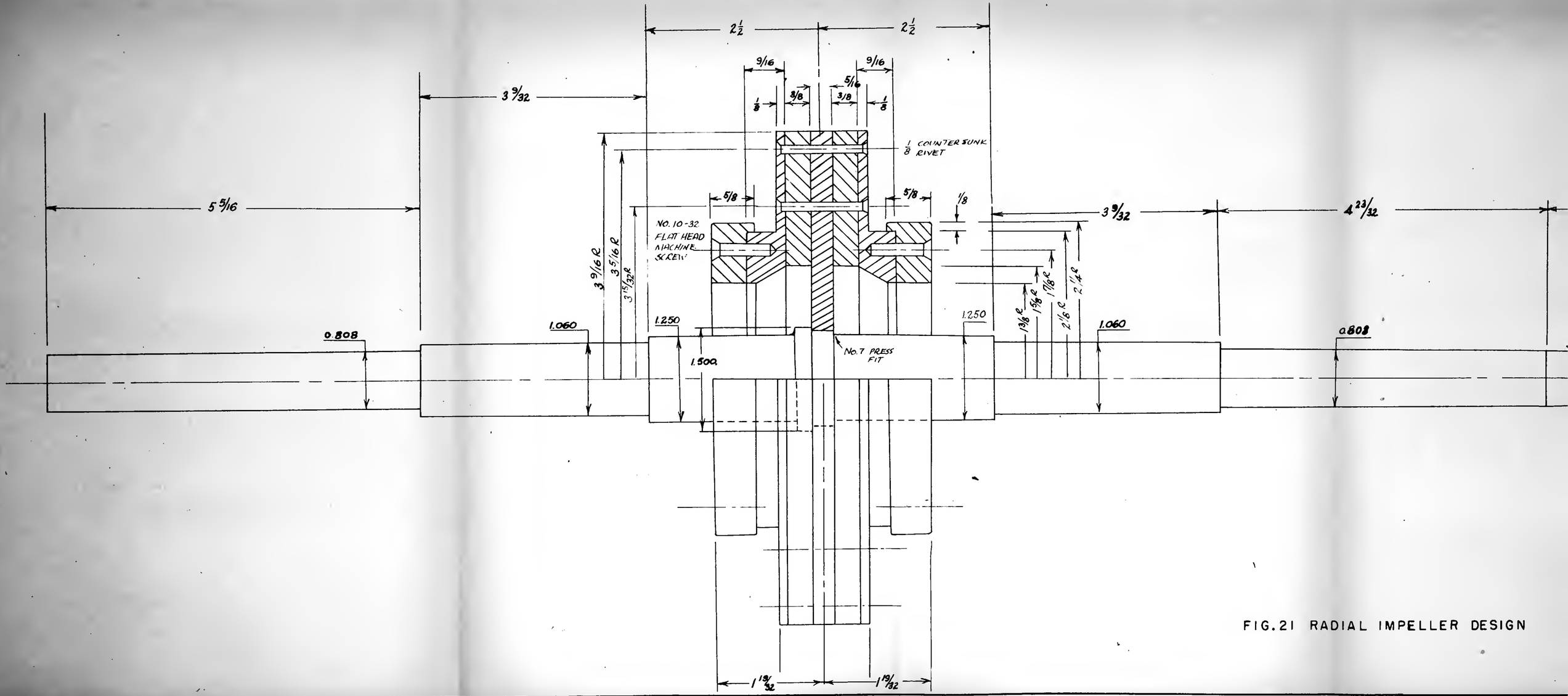

FIG. 21 RADIAL IMPELLER DESIGN

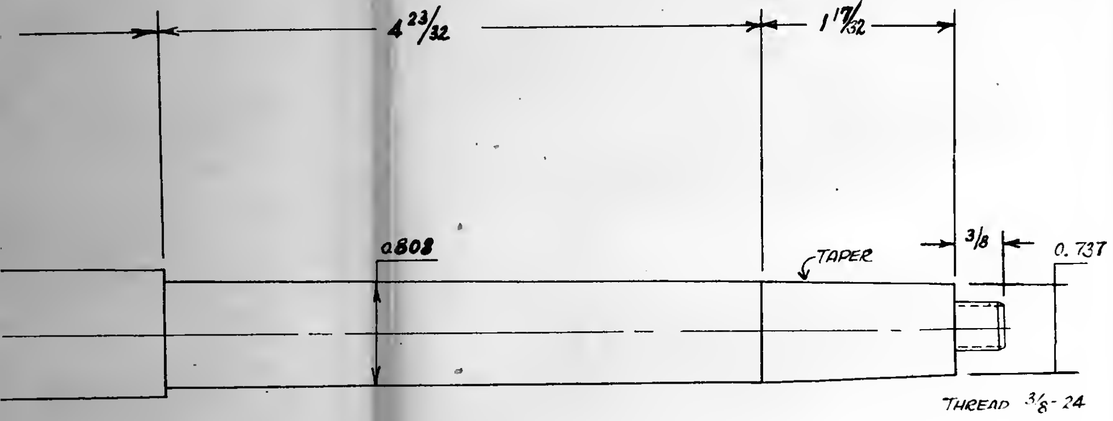

FIG. 21 RADIAL IMPELLER DESIGN

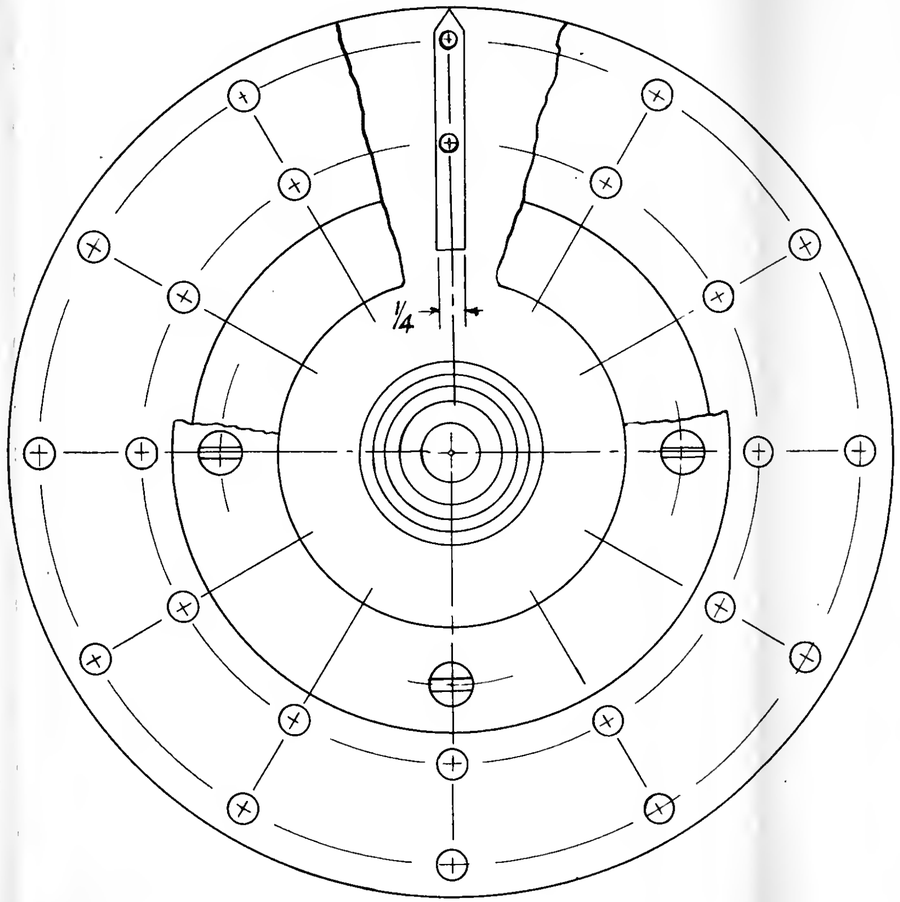

1	MATERIAL: 1020 STEEL/BRASS RINGS	1
	MASSACHUSETTS INSTITUTE OF TECHNOLOGY GAS TURBINE LABORATORY	
	CENTRIFUGAL RADIAL IMPELLER	
	R.E.B.	1 MAY 53
	J.F.B.	1" = 1"
		21

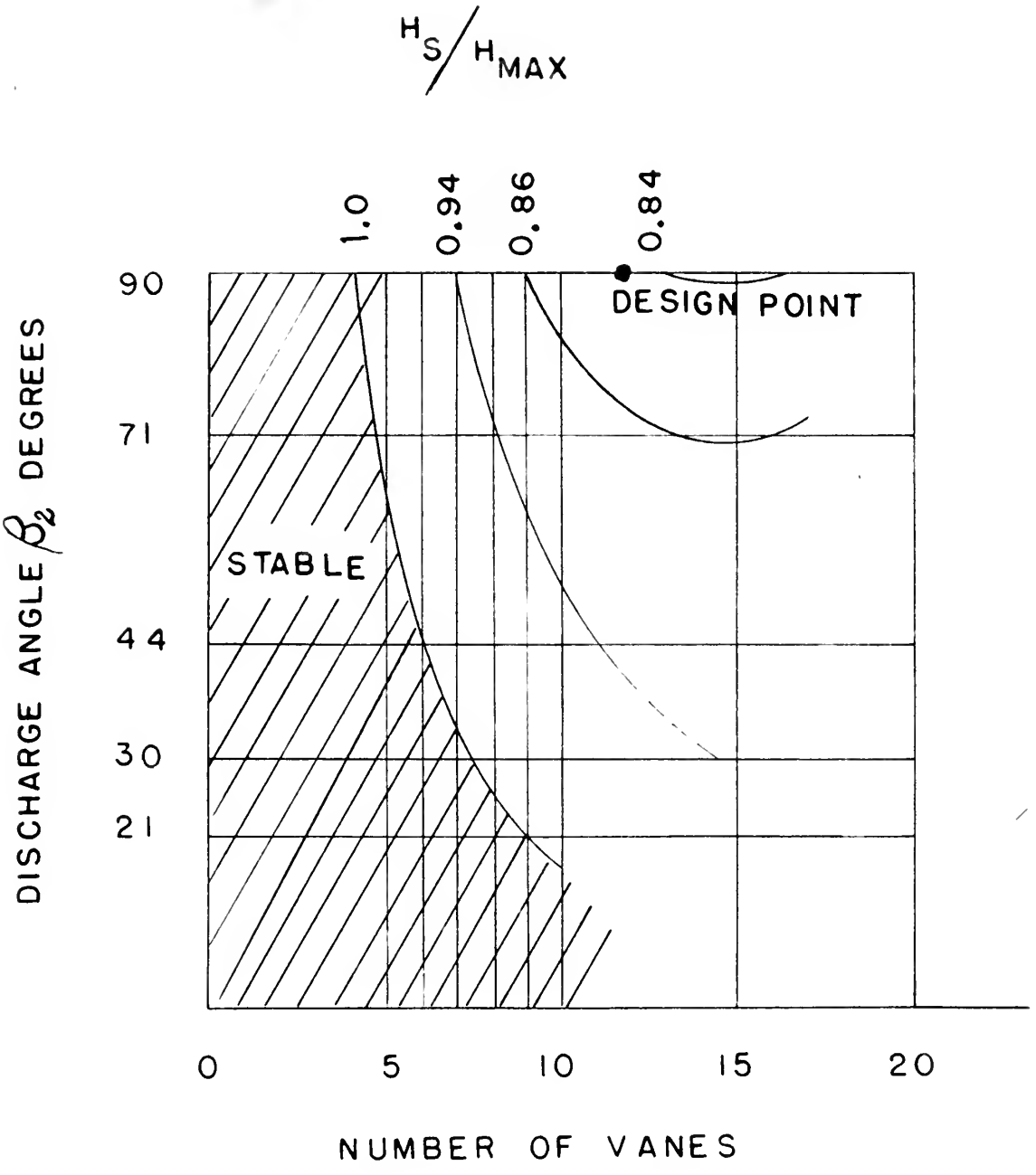

FIG. 22 CONDITIONS FOR A STABLE Q-H CURVE

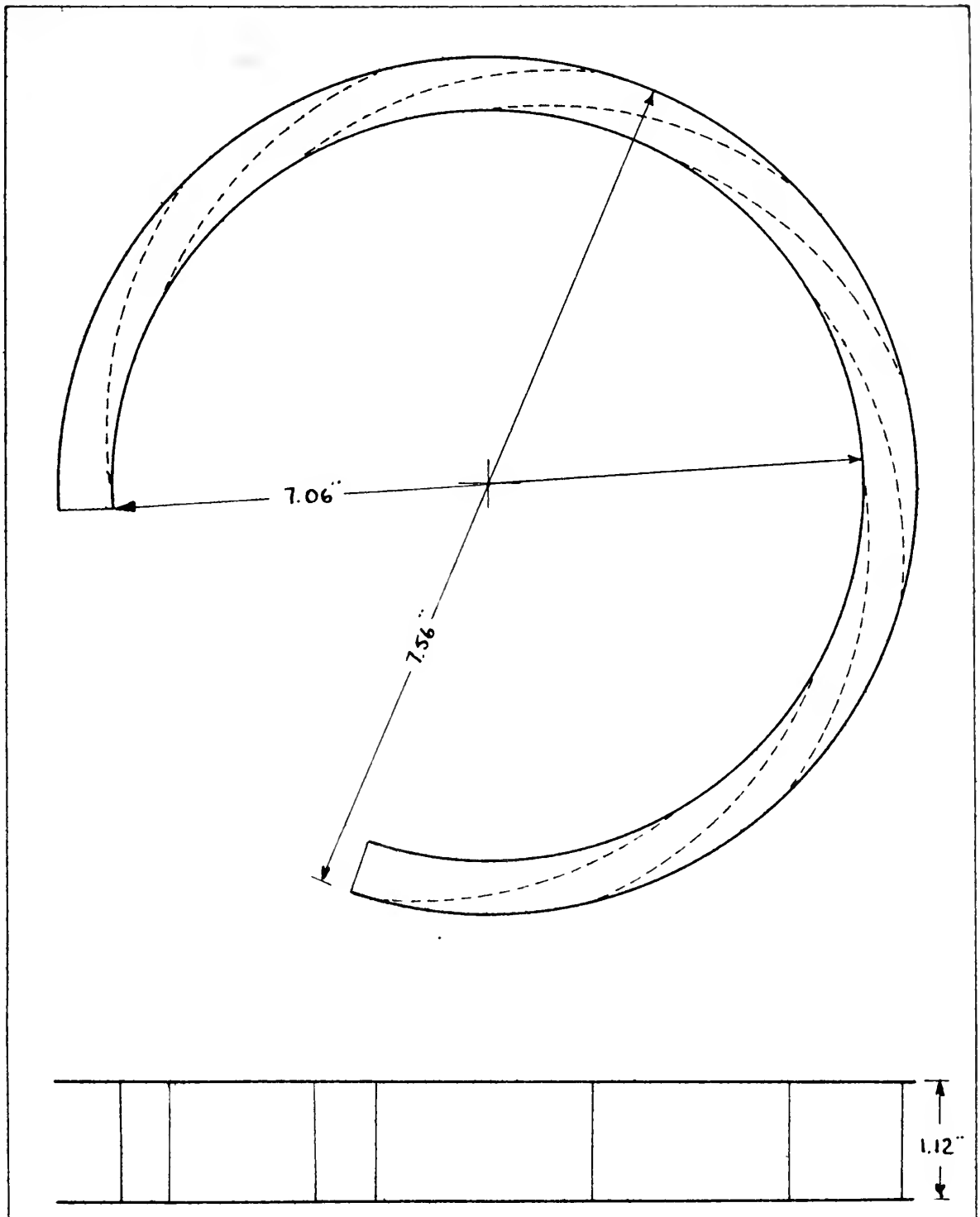

FIG. 23 DIFFUSER DESIGN

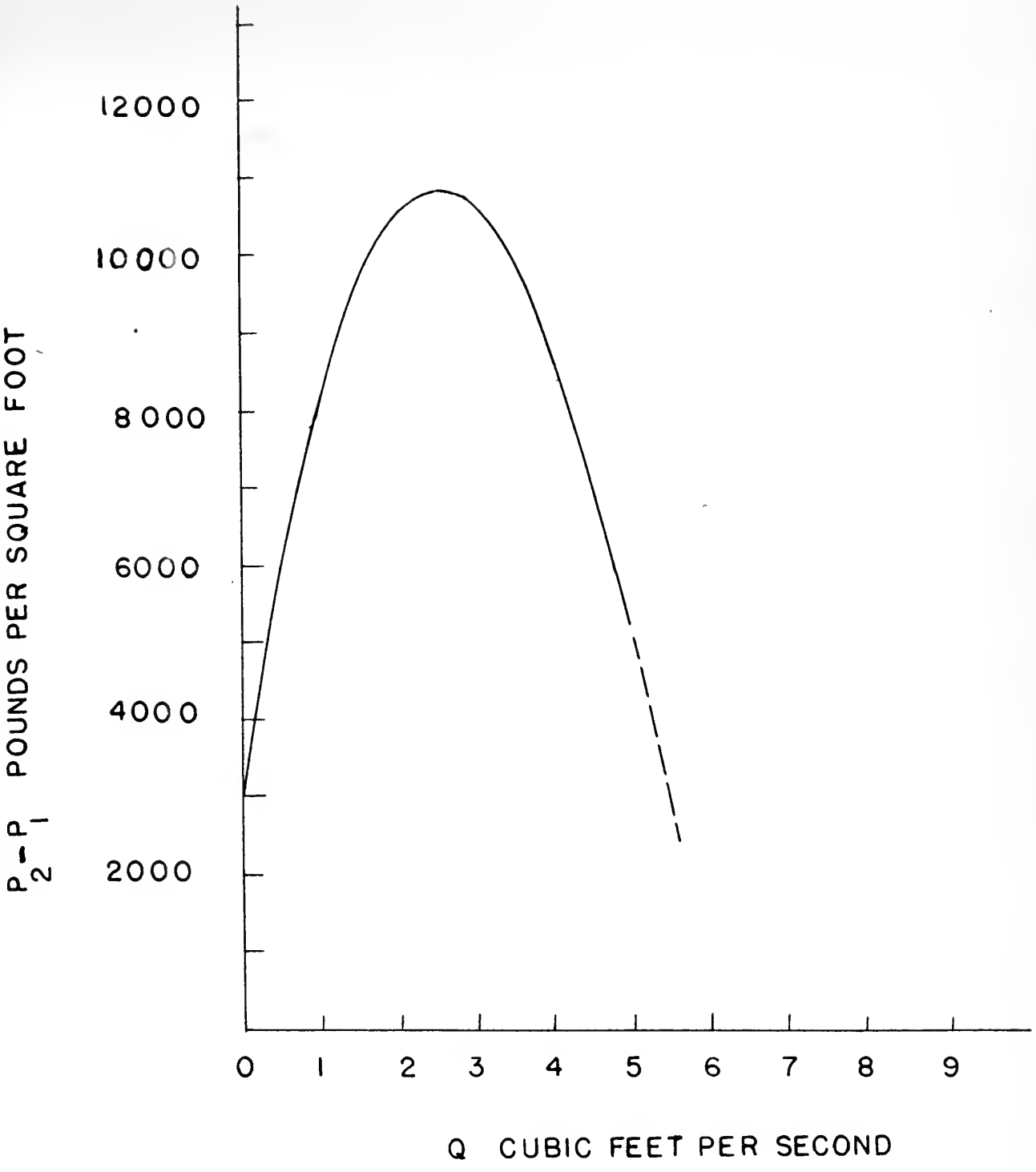

FIG. 24 THEORETICAL IMPELLER CHARACTERISTICS FORWARD BLADING

FIG. 25
EXPERIMENTAL RESULTS,
RADIAL VANED IMPELLER